PERIODIC TRAVELLING WAVES IN DIATOMIC GRANULAR CRYSTALS

PERIODIC TRAVELLING WAVES IN DIATOMIC GRANULAR CRYSTALS

By

MATTHEW BETTI, B.Sc.

A Thesis

Submitted to the School of Graduate Studies

in Partial Fulfillment of the Requirements

for the Degree

Master of Science

McMaster University

MASTER OF SCIENCE (2012)	McMaster University
(Mathematics)	Hamilton, Ontario

TITLE:	Periodic Travelling Waves in Diatomic Granular Crystals
AUTHOR:	Matthew Betti, B.Sc. (McMaster University)
SUPERVISOR:	Dr. Dmitry Pelinovsky
NUMBER OF PAGES:	vii, 91

Abstract

We study bifurcations of periodic travelling waves in granular dimer chains from the anti-continuum limit, when the mass ratio between the light and heavy beads tends to zero. We show that every limiting periodic wave is uniquely continued with respect to the mass ratio parameter and the periodic waves with the wavelength larger than a certain critical value are spectrally stable. Numerical computations are developed to study how this solution family is continued to the limit of equal mass ratio between the beads, where periodic travelling waves of granular monomer chains exist.

Acknowledgements

I owe sincere thanks to my supervisor Dr. Dmitry Pelinovsky for his continued support and patience, for openly sharing his knowledge of nonlinear wave equations with me, for remaining available for discussions, and for serving as a role model of what a good scientist and professor can be. I also express my gratitude to professors who taught me many things during lectures at McMaster University: Stanley Alama, Lia Bronsard, David Earn, Megumi Harada, Nicholas Kevlahan, Dmitry Pelinovsky, Bartosz Protas, Eric Sawyer, Partick Speissegger, Gail Wolkowicz, and Matthew Valeriote.

I also thank my family for their support, understanding and care.

To my parents,

Elvi and Silena

Contents

Introduction

Wave propagation in chains of granular crystals has been a popular area of study over the last decade. Granular crystals are realized physically as chains of densely packed, elastically interacting particles. These chains obey the Fermi-Pasta-Ulam (FPU) lattice equations, accompanied with Hertzian interaction forces. Experimental work with various materials based on granular crystals along with the many possible applications [6, 25] of such systems has motivated theoretical research on chains of granular crystals.

The existence of solitary waves in granular chains has been studied using several analytic and numerical techniques. MacKay [21] used the technique of Friesecke and Wattis [11] to prove the existence of solitary waves. Six years later, this result was used by English and Pego [9] to prove that spatial tails of such solitary waves have double-exponential decay. Numerically, Ahnert and Pikovsky [1] studied convergence to the solitary wave solution. In reviewing the variational technique of [11], Stefanov and Kevrekidis [27] proved that these solitary waves in granular chains are single-humped (bell-shaped).

The focus in this area of research has more recently shifted to periodic travelling waves in homogeneous and heterogeneous chains of granular crystals. This change in focus is due to the notion that such studies can be more relevant for physical experiments [13, 24]. James considers the existence of periodic

wave solutions of the differential advance-delay equation in the context of Newton's cradle [14] and homogeneous granular chains [15]. In [15], James shows the existence of periodic travelling waves in the neighbourhood of a special solution for binary oscillations using an application of the Implicit Function Theorem. Numerical calculations in [15] suggest that periodic waves with wavelength larger than a critical value are spectrally unstable. Numerical and asymptotic analysis in [15] also show the convergence to a solitary wave in the limit of infinite wavelength. More recent work [16] showed non-existence of time-periodic breathers in homogeneous granular crystals and existence of these breathers in Newton's cradle, where a discrete p-Schrödinger equation provides a robust approximation.

Starosvetsky *et al.* used numerical techniques based on Poincaré maps to approximate periodic waves in a chain of finitely many beads closed in a periodic loop. These waves were approximated both for monomers (homogeneous chains) [26] and dimers (chains of beads of alternating masses) [17]. Solitary waves were found to exist in the limit of an infinite mass ratio between light and heavy particles in [17]. The authors of [17] explain that such solitary waves are in resonance with linear waves and therefore do not persist when changing the mass ratio parameter. The existence of a countable set of mass ratio parameters for which solitary waves should exist are suggested by numerical results in [17], yet no rigorous studies of this problem have been developed. Recent work [18] contains numerical results on existence of periodic travelling waves in granular dimer chains.

This thesis is devoted to analysis of periodic travelling waves in dimer granular chains. In particular:

- We use the anti-continuum limit of the FPU lattice, recently explored in

the context of existence and stability of discrete multi-site breathers by Yoshimura [28], to find a periodic travelling wave solution to the dimer system in the anti-continuum limit.

- From the solution at the anti-continuum limit, we use a variation of the Implicit Function Theorem to prove that every limiting periodic travelling wave is uniquely continued with respect to the mass-ratio parameter. These results differ from the asymptotic calculations in [17], where a different limiting solution is considered in the anti-continuum limit.

- We use perturbation arguments, similar to those developed in [23], to determine spectral stability of periodic travelling waves. We show that periodic travelling waves with wavelength larger than a certain critical value are spectrally stable.

- We show numerically that the family of periodic travelling waves bifurcating from the anti-continuum limit extend to the limit of equal masses for the dimer chains. We also show numerically that the periodic travelling waves of the homogeneous chains considered in [15] are different than those extended to the equal mass limit from the anti-continuum limit. In other words, the periodic waves in dimers do not satisfy the reductions to periodic waves of monomer chains even at the equal mass-ratio limit.

This thesis is organized as follows: Chapter 1 introduces the model and sets up the necessary preliminaries for the search of periodic travelling waves. Chapter 2 develops a continuation of periodic travelling waves from the anti-continuum limit. Perturbative arguments that characterize Floquet multipliers to determine spectral stability of periodic travelling waves near the anti-continuum limit are discussed in Chapter 3. Numerical results are

collected in Chapter 4. The MATLAB codes used for numerical computations are collected at the end of the thesis.

Chapter 1

Mathematical Formalism

1.1 The Model

We consider an infinite chain of spherical beads of alternating masses (a *dimer*), which obey Newton's equations of motion,

$$\begin{cases} m\ddot{x}_n = V'(y_n - x_n) - V'(x_n - y_{n-1}), \\ M\ddot{y}_n = V'(x_{n+1} - y_n) - V'(y_n - x_n), \end{cases} \quad n \in \mathbb{Z}, \tag{1.1}$$

where m and M represent masses such that $m \leq M$. $\{x_n\}_{n\in\mathbb{Z}}$ and $\{y_n\}_{n\in\mathbb{Z}}$ are the coordinates of the centres of the beads of mass m and M, respectively. V is the interaction potential that represents the Hertzian contact forces for perfect spheres [24, 25]:

$$V(x) = \frac{1}{1+\alpha}|x|^{1+\alpha}H(-x) \tag{1.2}$$

where $\alpha = \frac{3}{2}$ and H is the Heaviside step function with $H(x) = 1$ for $x > 0$ and $H(x) = 0$ for $x \leq 0$. The value of α is determined by the spherical geometry

of the beads. The Heaviside function with a negative argument captures the behaviour that the beads will only experience a force when in contact with one another and will move inertially when not in contact with another bead.

Making the substitution,

$$n \in \mathbb{Z}: \quad x_n(t) = u_{2n-1}(\tau), \quad y_n(t) = \varepsilon w_{2n}(\tau), \quad t = \sqrt{m}\tau \tag{1.3}$$

where $\varepsilon^2 = \frac{m}{M}$, we can rewrite the system of Newton's equations (1.1) as

$$\begin{cases} \ddot{u}_{2n-1} = V'(\varepsilon w_{2n} - u_{2n-1}) - V'(u_{2n-1} - \varepsilon w_{2n-2}), \\ \ddot{w}_{2n} = \varepsilon V'(u_{2n+1} - \varepsilon w_{2n}) - \varepsilon V'(\varepsilon w_{2n} - u_{2n-1}), \end{cases} \quad n \in \mathbb{Z}. \tag{1.4}$$

The limit $\varepsilon = 0$ is referred to as the anti-continuum limit of zero mass ratio. In the limit of equal masses that is, for $\varepsilon = 1$, we can apply the reduction,

$$n \in \mathbb{Z}: \quad u_{2n-1}(\tau) = U_{2n-1}(\tau), \quad w_{2n}(\tau) = U_{2n}(\tau). \tag{1.5}$$

Under this substitution, the system of two granular chains (1.4) reduces to the scalar system of Newton's equation of motion that describes a homogeneous chain of granular crystals of uniform mass (a *monomer*),

$$\ddot{U}_n = V'(U_{n+1} - U_n) - V'(U_n - U_{n-1}), \quad n \in \mathbb{Z}. \tag{1.6}$$

We note two symmetries of the dimer equation (1.4). The first is translational invariance of solutions with respect to τ. If $\{u_{2n-1}(\tau),\, w_{2n}(\tau)\}_{n\in\mathbb{Z}}$ is a solution of (1.4) then

$$\{u_{2n-1}(\tau + b),\, w_{2n}(\tau + b)\}_{n\in\mathbb{Z}} \tag{1.7}$$

is also a solution for any $b \in \mathbb{R}$. The second symmetry is a uniform shift of the coordinates $\{u_{2n-1}(\tau),\, w_{2n}(\tau)\}_{n\in\mathbb{Z}}$ in the direction of $(\varepsilon, 1)$. If $\{u_{2n-1}(\tau),\, w_{2n}(\tau)\}_{n\in\mathbb{Z}}$ is a solution of (1.4), then

$$\{u_{2n-1}(\tau) + \varepsilon a,\, w_{2n}(\tau) + a\}_{n\in\mathbb{Z}} \tag{1.8}$$

is also a solution for any $a \in \mathbb{R}$.

The Hamiltonian function for system (1.4) is given by

$$H = \frac{1}{2}\sum_{n\in\mathbb{Z}}(p_{2n-1}^2 + q_{2n}^2) + \sum_{n\in\mathbb{Z}} V(\varepsilon w_{2n} - u_{2n-1}) + \sum_{n\in\mathbb{Z}} V(u_{2n-1} - \varepsilon w_{2n-2}), \tag{1.9}$$

written in canonical variables $\{u_{2n-1}, p_{2n-1} = \dot{u}_{2n-1}, w_{2n}, q_{2n} = \dot{w}_{2n}\}$. With the Hamiltonian (1.9), we can write the system (1.4) via the symplectic structure:

$$\dot{u}_{2n-1} = \frac{\partial H}{\partial p_{2n-1}}, \quad \dot{p}_{2n-1} = \frac{\partial H}{\partial u_{2n-1}}, \quad \dot{w}_{2n} = \frac{\partial H}{\partial q_{2n}}, \quad \dot{q}_{2n} = \frac{\partial H}{\partial w_{2n}}. \tag{1.10}$$

1.2 Periodic Travelling Waves

In this thesis, we consider 2π-periodic solutions of the system (1.4). In other words, we consider solutions such that,

$$u_{2n-1}(\tau) = u_{2n-1}(\tau + 2\pi), \quad w_{2n}(\tau) = w_{2n}(\tau + 2\pi), \quad \tau \in \mathbb{R}, \quad n \in \mathbb{Z}. \tag{1.11}$$

In addition to this requirement, we consider travelling wave solutions that satisfy the reduction,

$$u_{2n+1}(\tau) = u_{2n-1}(\tau + 2q), \quad w_{2n+2}(\tau) = w_{2n}(\tau + 2q), \quad \tau \in \mathbb{R}, \quad n \in \mathbb{Z}, \tag{1.12}$$

where $q \in [0, \pi]$ is a free parameter. Given constraints (1.11) and (1.12) for periodic travelling wave solutions, there must exist 2π-periodic functions u_* and w_* such that

$$u_{2n-1}(\tau) = u_*(\tau + 2qn), \quad w_{2n}(\tau) = w_*(\tau + 2qn), \quad \tau \in \mathbb{R}, \quad n \in \mathbb{Z}. \quad (1.13)$$

Parameter q is inversely proportional to the wavelength of the periodic wave when regarded in this context. The functions u_* and w_* satisfy a system of advance-delay differential equations:

$$\begin{cases} \ddot{u}_*(\tau) = V'(\varepsilon w_*(\tau) - u_*(\tau)) - V'(u_*(\tau) - \varepsilon w_*(\tau - 2q)), \\ \ddot{w}_*(\tau) = \varepsilon V'(u_*(\tau + 2q) - \varepsilon w_*(\tau)) - \varepsilon V'(\varepsilon w_*(\tau) - u_*(\tau)), \end{cases} \quad \tau \in \mathbb{R}. \quad (1.14)$$

Remark 1. *We could generalize the class of solutions by seeking a periodic travelling wave in the form*

$$u_{2n-1}(\tau) = u_*(c\tau + 2qn), \quad w_{2n}(\tau) = w_*(c\tau + 2qn), \quad \tau \in \mathbb{R}, \quad n \in \mathbb{Z},$$

where $c > 0$ is an arbitrary parameter. With the help of a scaling transformation of system (1.4)*, we can always normalize c to one.*

Remark 2. *It will be useful for numerical approximations and stability analysis of periodic travelling waves to consider another reduction. For particular values, $q = \frac{m\pi}{N}$, where $1 \leq m \leq N$, we can reduce system* (1.4) *to a system of $2mN$ second-order ordinary differential equations subject to the periodic boundary conditions:*

$$u_{-1} = u_{2mN-1}, \quad u_{2mN+1} = u_1, \quad w_0 = w_{2mN}, \quad w_{2mN+2} = w_2. \quad (1.15)$$

1.3 The Anti-Continuum Limit

The anti-continuum limit occurs when mass M is infinitely larger than mass m, so that $\varepsilon = 0$. In this limit, the system of differential-advance delay equations, (1.14) reduces to:

$$\begin{cases} \ddot{u}_*(\tau) = V'(-u_*(\tau)) - V'(u_*(\tau)), \\ \ddot{w}_*(\tau) = 0, \end{cases} \qquad \tau \in \mathbb{R}. \tag{1.16}$$

We can see that the system is decoupled in the anti-continuum limit and the equation for u_* can be further simplified,

$$\begin{aligned} \ddot{u}_*(\tau) &= V'(-u_*(\tau)) - V'(u_*(\tau)) \\ &= -|u_*(\tau)|^{\alpha} H(u_*(\tau)) + |u_*(\tau)|^{\alpha} H(-u_*(\tau)) \\ &= -|u_*(\tau)|^{\alpha-1} u_*(\tau) \end{aligned}$$

Let φ be a solution of the nonlinear oscillator equation,

$$\ddot{\varphi} = V'(-\varphi) - V'(\varphi) \quad \rightarrow \quad \ddot{\varphi} + |\varphi|^{\alpha-1}\varphi = 0. \tag{1.17}$$

Since $\alpha = \frac{3}{2}$, the fourth derivative of φ is no longer continuous in t. Thus, if φ is a 2π-periodic solution to equation (1.17), then $\varphi \in C^3_{per}(0, 2\pi)$.

The nonlinear oscillator (1.17) has the first integral (or energy),

$$E = \frac{1}{2}\dot{\varphi}^2 + \frac{1}{1+\alpha}|\varphi|^{\alpha+1}. \tag{1.18}$$

The phase portrait of the nonlinear oscillator, (1.17), in the $(\varphi, \dot{\varphi})$-plane

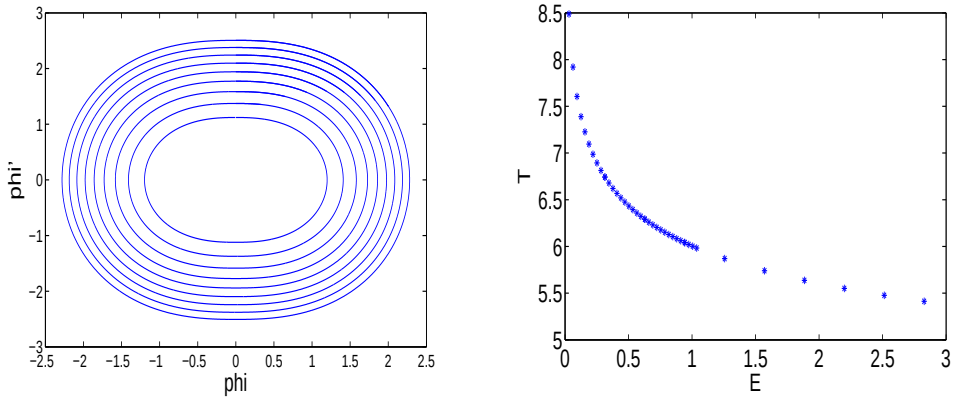

Figure 1.1: Left: Phase portrait of the nonlinear oscillator (1.17) in the $(\varphi, \dot{\varphi})$-plane. Right: The period T of the nonlinear oscillator versus energy E.

consists of a family of closed orbits around the point $(0, 0)$. This is visualized numerically in Figure 1.1 (left). It is clear that the origin is the only critical point for equation (1.17). Each orbit corresponds to a T-periodic solution, φ, where T is determined uniquely by the energy E. It is known [15, 28] that for $\alpha > 1$ the period T is a monotonically decreasing function of E with the properties that $T \to \infty$ as $E \to 0$ and $T \to 0$ as $E \to \infty$. Figure 1.1 (right) verifies this numerically for the nonlinear oscillator, (1.17). Given these properties, we can conclude that there is a unique $E_0 > 0$ such that $T(E_0) = 2\pi$. We also know that the nonlinear oscillator (1.17) is nondegenerate in the sense that $T'(E_0) \neq 0$. More precisely, $T'(E_0) < 0$.

In this thesis, we consider only 2π-periodic functions φ, defined by (1.18) for $E = E_0$. We define a unique φ by fixing the initial conditions at $\varphi(0) = 0$ and $\dot{\varphi}(0) > 0$. These initial conditions uniquely determine one of two odd solutions, φ, to equation (1.17).

Using equations (1.16) and (1.17), we conclude that the limiting 2π-periodic travelling wave solutions at $\varepsilon = 0$ which satisfy the constraints (1.12)

for any fixed $q \in [0, \pi]$ are

$$\varepsilon = 0: \quad u_{2n-1}(\tau) = \varphi(\tau + 2qn), \quad w_{2n}(\tau) = 0, \quad \tau \in \mathbb{R}, \quad n \in \mathbb{Z}. \tag{1.19}$$

We will prove persistence of the limiting solutions (1.19) in powers of ε in the granular dimer chain (1.4). To do this, we will work in the Sobolev space of odd 2π-periodic functions for $\{u_{2n-1}\}_{n\in\mathbb{Z}}$,

$$H^k_u = \left\{ u \in H^k_{\rm per}(0, 2\pi): \quad u(-\tau) = -u(\tau), \ \tau \in \mathbb{R} \right\}, \quad k \in \mathbb{N}_0, \tag{1.20}$$

and in the Sobolev space of 2π-periodic functions with zero mean for $\{w_{2n}\}_{n\in\mathbb{Z}}$,

$$H^k_w = \left\{ w \in H^k_{\rm per}(0, 2\pi): \quad \int_0^{2\pi} w(\tau) d\tau = 0 \right\}, \quad k \in \mathbb{N}_0. \tag{1.21}$$

The choice of spaces is motivated by the symmetries (1.7) and (1.8). The two symmetries generate a two dimensional kernel of the linearized operators of the system (1.4). The choice of constraints in (1.20) and (1.21) creates a trivial, zero-dimensional kernel for the linearized operators. We will see more on the linearized operators and their kernels in the following chapter.

It will be clear from analysis that the vector space defined in (1.21) is not precise enough to prove the persistence of travelling wave solutions satisfying constraints (1.12). Therefore we will need a more precise space given by,

$$\tilde{H}^k_w = \left\{ w \in H^k_{per}(0, 2\pi): \quad w(\tau) = -w(-\tau - 2q) \right\}, \quad k \in \mathbb{N}_0. \tag{1.22}$$

We can see clearly that $\tilde{H}^k_w \subset H^k_w$ since if w is a 2π-periodic function, then

$$\begin{aligned}\int_0^{2\pi} w(\tau)d\tau &= -\int_0^{2\pi} w(-\tau-2q)d\tau \\ &= \int_{-2q}^{-2\pi-2q} w(\tau)d\tau \\ &= -\int_0^{2\pi} w(\tau)d\tau,\end{aligned}$$

from which we conclude that $\int_0^{2\pi} w(\tau)d\tau = 0$.

1.4 Special Periodic Travelling Waves

In the next chapter, we shall prove persistence of periodic travelling wave solutions from the anti-continuum limit for $\varepsilon > 0$. It is worthwhile to mention before such analysis the existence of three explicit periodic travelling wave solutions of the granular dimer chain (1.4) for special values of q.

The simplest of these solutions occurs at $q = \frac{\pi}{2}$. Setting $w_* = 0$, the system (1.14) reduces to

$$\begin{cases} \ddot{u}_*(\tau) = V'(-u_*(\tau)) - V'(u_*(\tau)), \\ 0 = V'(u_*(\tau+\pi)) - V'(-u_*(\tau)), \end{cases} \quad \tau \in \mathbb{R}. \tag{1.23}$$

The solution, φ of the nonlinear oscillator (1.17) has the symmetry

$$\varphi(\tau-\pi) = \varphi(\tau+\pi) = -\varphi(\tau).$$

Therefore, we obtain the exact solution $u_* = \varphi$ that gives:

$$q = \frac{\pi}{2}: \quad u_{2n-1}(\tau) = \varphi(\tau + n\pi), \quad w_{2n}(\tau) = 0 \tag{1.24}$$

For $q = 0$ and $q = \pi$, the system (1.14) reduces to,

$$\begin{cases} \ddot{u}_*(\tau) = V'(\varepsilon w_*(\tau) - u_*(\tau)) - V'(u_*(\tau) - \varepsilon w_*(\tau)), \\ \ddot{w}_*(\tau) = \varepsilon V'(u_*(\tau) - \varepsilon w_*(\tau)) - \varepsilon V'(\varepsilon w_*(\tau) - u_*(\tau)), \end{cases} \quad \tau \in \mathbb{R}. \tag{1.25}$$

Under the change of variables $p(\tau) = u_*(\tau) - \varepsilon w_*(\tau)$ we can reduce the system to,

$$\begin{cases} \ddot{p}(\tau) = (1+\varepsilon^2)(V'(-p(\tau)) - V'(p(\tau)) \\ \ddot{u}_*(\tau) = V'(-p(\tau)) - V'(p(\tau)), \end{cases} \quad \tau \in \mathbb{R}. \tag{1.26}$$

This provides the exact solution $p = \frac{\varphi}{(1+\varepsilon^2)^2}$, that gives,

$$q = \{0, \pi\}: \quad u_{2n-1}(\tau) = \frac{\varphi(\tau)}{(1+\varepsilon^2)^3}, \quad w_{2n}(\tau) = \frac{-\varepsilon\varphi(\tau)}{(1+\varepsilon^2)^3}. \tag{1.27}$$

By construction, the solutions (1.24) and (1.27) persist for any $\varepsilon \geq 0$. In the following chapter, we investigate whether the continuations are unique near $\varepsilon = 0$ for the special values of q, as well as whether the general limiting solution (1.19) can be continued uniquely in ε for any other fixed value of $q \in [0, \pi]$.

It is worthwhile to note that the exact solution (1.27) at $q = \pi$ and $\varepsilon = 1$ satisfies the monomer constraint (1.5) in that

$$U_{2n-1}(\tau) = -U_{2n}(\tau) = U_{2n}(\tau - \pi).$$

This reduction shows that the solution at $\varepsilon = 1, q = \pi$ satisfies the granular monomer chain (1.6) and coincides with the solution obtained by James [15]. In contrast, the solutions (1.24) and (1.27) for $q = 0$ do not satisfy the monomer constraints (1.5) at $\varepsilon = 1$. This would suggest that there exist two distinct solutions at $\varepsilon = 1$ for $q \neq \pi$. One is continued from $\varepsilon = 0$ and the other one

is constructed from the solution of the monomer chain (1.6) in [15].

Chapter 2

Persistence of Periodic Travelling Waves Near $\varepsilon = 0$

2.1 Existence and Uniqueness Result

We consider the system of differential advance-delay equations (1.14). The limiting solution to equations (1.14) is given by,

$$\varepsilon = 0 : \quad u_*(\tau) = \varphi(\tau), \quad w_*(\tau) = 0, \quad \tau \in \mathbb{R}, \tag{2.1}$$

where φ is a unique odd 2π-periodic solution to the nonlinear oscillator equation (1.17) with $\dot{\varphi}(0) > 0$.

The aim of this chapter is to prove a unique continuation of (2.1) for $\varepsilon > 0$. The following theorem summarizes the main result.

Theorem 1. *Fix $q \in [0, \pi]$. There is a unique C^1 continuation of 2π-periodic travelling wave (2.1) in ε. In other words, there is an $\varepsilon_0 > 0$ such that for all $\varepsilon \in (0, \varepsilon_0)$ there exist a positive constant C and a unique solution $(u_*, w_*) \in$*

$H_u^2 \times \tilde{H}_w^2$ *of the system of differential advance-delay equations* (1.14) *such that*

$$\|u_* - \varphi\|_{H^2_{\rm per}} \leq C\varepsilon^2, \quad \|w_*\|_{H^2_{\rm per}} \leq C\varepsilon. \tag{2.2}$$

Remark 3. *By Theorem 1, the limiting solution* (2.1) *for* $q \in \left\{0, \frac{\pi}{2}, \pi\right\}$ *is uniquely continued for any* $\varepsilon > 0$ *as exact solutions* (1.24) *and* (1.27)*.*

2.2 Formal Expansions in ε

Before proving Theorem 1, we first attempt formal expansions in powers of ε to understand the persistence analysis from $\varepsilon = 0$. Since V is C^2 but not C^3, the formal power series expansion in ε cannot be continued beyond the power of ε^2.

We expand the solution of the differential advance-delay equations (1.14) as follows,

$$u_*(\tau) = \varphi(\tau) + \varepsilon^2 u_*^{(2)}(\tau) + \mathrm{o}(\varepsilon^2), \quad w_*(\tau) = \varepsilon w_*^{(1)}(\tau) + \mathrm{o}(\varepsilon^2). \tag{2.3}$$

From these expansions, we can obtain the linear inhomogeneous equations for $u_*^{(2)}$ and $w_*^{(1)}$, given by:

$$\ddot{w}_*^{(1)}(\tau) = F_w^{(1)}(\tau) := V'(\varphi(\tau + 2q)) - V'(-\varphi(\tau)) \tag{2.4}$$

and

$$\ddot{u}_*^{(2)}(\tau) + \alpha|\varphi(\tau)|^{\alpha-1} u_*^{(2)}(\tau) = F_u^{(2)}(\tau) := V''(-\varphi(\tau))w_*^{(1)}(\tau) + V''(\varphi(\tau))w_*^{(1)}(\tau - 2q). \tag{2.5}$$

We consider the two differential operators

$$L_0 = \frac{d^2}{d\tau^2} \quad : \qquad H^2_{\text{per}}(0, 2\pi) \to L^2_{\text{per}}(0, 2\pi), \tag{2.6}$$

$$L = \frac{d^2}{d\tau^2} + \alpha|\varphi(\tau)|^{\alpha-1} \quad : \qquad H^2_{\text{per}}(0, 2\pi) \to L^2_{\text{per}}(0, 2\pi), \tag{2.7}$$

These operators are not invertible in $L^2_{\text{per}}(0, 2\pi)$ because they admit one-dimensional kernels,

$$\text{Ker}(L_0) = \text{span}\{1\}, \quad \text{Ker}(L) = \text{span}\{\dot{\varphi}\}. \tag{2.8}$$

The kernel of L is one-dimensional so long as the system is non-degenerate, i.e. $T'(E_0) \neq 0$ [15].

To find unique solutions to the inhomogeneous equations (2.4) and (2.5) in the function spaces H^2_w (1.21) and H^2_u (1.20) respectively, the source terms $F^{(1)}_w$ and $F^{(2)}_u$ must satisfy the Fredholm conditions [10]:

$$\langle 1, F^{(1)}_w \rangle_{L^2_{\text{per}}} = 0 \quad \text{and} \quad \langle \dot{\varphi}, F^{(2)}_u \rangle_{L^2_{\text{per}}} = 0. \tag{2.9}$$

The first Fredholm condition is expanded as

$$\begin{aligned} \langle 1, F^{(1)}_w \rangle_{L^2_{\text{per}}} &= \int_0^{2\pi} \left[V'(\varphi(\tau + 2q)) - V'(-\varphi(\tau)) \right] d\tau \\ &= \int_0^{2\pi} V'(\varphi(\tau + 2q)) d\tau - \int_0^{2\pi} V'(-\varphi(\tau)) d\tau \\ &= 0. \end{aligned}$$

The third equality holds because the mean value of a periodic function is independent of the limits of integration so long as we integrate over a full period. Therefore, the first Fredholm condition is satisfied.

The second Fredholm condition is given by

$$\langle \dot{\varphi}, F_u^{(2)} \rangle_{L^2_{\text{per}}} = \int_0^{2\pi} \dot{\varphi}(\tau) \left[V''(-\varphi(\tau)) w_*^{(1)}(\tau) + V''(\varphi(\tau)) w_*^{(1)}(\tau - 2q) \right] d\tau = 0.$$

The second Fredholm condition is satisfied if $F_u^{(2)}$ is odd in τ since we are taking the integral over a full period and $\dot{\varphi}$ is even in τ. We show that $F_u^{(2)}$ is odd in τ by proving

$$w_*^{(1)}(\tau) = -w_*^{(1)}(-\tau - 2q), \quad \Rightarrow \quad F_u^{(2)}(-\tau) = -F_u^{(2)}(\tau), \quad \tau \in \mathbb{R}. \tag{2.10}$$

Indeed, using equation (2.4) we show that

$$\begin{aligned} \ddot{w}_*^{(1)}(\tau) + \ddot{w}_*^{(1)}(-\tau - 2q) &= V'(\varphi(\tau + 2q)) - V'(-\varphi(\tau)) \\ &\quad + V'(\varphi(-\tau)) - V'(-\varphi(-\tau - 2q)) \\ &= 0, \end{aligned}$$

where the second equality holds because φ is odd in τ. Integrating this equation twice yields,

$$w_*^{(1)}(\tau) + w_*^{(1)}(-\tau - 2q) = 0,$$

since $w_*^{(1)} \in H^2_w$. This condition gives,

$$\begin{aligned} F_u^{(2)}(\tau) &= V''(-\varphi(\tau)) w_*^{(1)}(\tau) + V''(\varphi(\tau)) w_*^{(1)}(\tau - 2q) \\ &= V''(-\varphi(\tau)) w_*^{(1)}(\tau) - V''(\varphi(\tau)) w_*^{(1)}(-\tau) \\ &= -F_u^{(2)}(-\tau), \end{aligned}$$

and reduction (2.10) is proved. Therefore we can conclude that the second Fredholm condition is satisfied. The sufficient condition on $w_*^{(1)}$, needed to

prove the second Fredholm condition, suggests the need to use $\tilde{H}^2_w$ instead of H^2_w, where $\tilde{H}^2_w$ is given by (1.22).

We see that up to $\mathcal{O}(\varepsilon^2)$ a unique solution exists. However, this formal method cannot be used to expand to arbitrary order in powers of ε due to the lack of regularity of the potential, V. In the following section we prove Theorem 1 by means of the implicit function theorem.

2.3 Proof of Theorem 1

To prove Theorem 1, we shall consider the vector fields of the system of differential advance-delay equations (1.14),

$$\begin{cases} F_u(u(\tau), w(\tau), \varepsilon) := V'(\varepsilon w(\tau) - u(\tau)) - V'(u(\tau) - \varepsilon w(\tau - 2q)), \\ F_w(u(\tau), w(\tau), \varepsilon) := \varepsilon V'(u(\tau + 2q) - \varepsilon w(\tau)) - \varepsilon V'(\varepsilon w(\tau) - u(\tau)), \end{cases} \quad \tau \in \mathbb{R}. \tag{2.11}$$

We seek a strong solution $(u_*, w_*) \in H^2_u \times \tilde{H}^2_w$ of system (1.14) satisfying the conditions,

$$u_*(-\tau) = -u_*(\tau), \quad w_*(\tau) = -w_*(-\tau - 2q), \quad \tau \in \mathbb{R}. \tag{2.12}$$

We first note that F_u is odd in τ if $(u, w) \in H^2_u \times \tilde{H}^2_w$:

$$\begin{aligned} F_u(u(\tau), w(\tau), \varepsilon) &= V'(\varepsilon w(\tau) - u(\tau)) - V'(u(\tau) - \varepsilon w(\tau - 2q)) \\ &= V'(-\varepsilon w(-\tau - 2q) + u(-\tau)) - V'(-u(-\tau) + \varepsilon w(-\tau)) \\ &= -F_u(u(-\tau), w(-\tau), \varepsilon). \end{aligned}$$

As well, since $V \in C^2$, F_u is a C^1 map from $H^2_u \times \tilde{H}^2_w \times \mathbb{R} \to L^2_u$ and the

Jacobian of F_u at $\varepsilon = 0$ is given by

$$D_u F_u(u, w, 0) = V''(-u) - V''(u) = -\alpha|u|^{\alpha-1}, \quad D_w F_u(u, w, 0) = 0. \quad (2.13)$$

Next, under the constraints (2.12), we have $F_w \in \tilde{L}^2_w$ because

$$\begin{aligned} &F_w(u(\tau), w(\tau), \varepsilon) + F_w(u(-\tau - 2q), w(-\tau - 2q), \varepsilon) \\ &\quad = \varepsilon V'(u(\tau + 2q) - \varepsilon w(\tau)) - \varepsilon V'(\varepsilon w(\tau) - u(\tau)) \\ &\qquad + \varepsilon V'(u(-\tau) - \varepsilon w(-\tau - 2q)) \\ &\qquad - \varepsilon V'(\varepsilon w(-\tau - 2q) - u(-\tau - 2q)) \\ &\quad = 0. \end{aligned}$$

Since V is C^2, F_w is a C^1 map from $H^2_u \times \tilde{H}^2_w \times \mathbb{R} \to \tilde{L}^2_w$ and its Jacobian at $\varepsilon = 0$ is given by

$$D_u F_w(u, w, 0) = 0, \quad D_w F_w(u, w, 0) = 0. \quad (2.14)$$

We now define the nonlinear operator

$$\begin{cases} f_u(u, w, \varepsilon) := \frac{d^2 u}{d\tau^2} - F_u(u, w, \varepsilon), \\ f_w(u, w, \varepsilon) := \frac{d^2 w}{d\tau^2} - F_w(u, w, \varepsilon). \end{cases} \quad (2.15)$$

We have $(f_u, f_w) : H^2_u \times \tilde{H}^2_w \times \mathbb{R} \to L^2_u \times \tilde{L}^2_w$ because the second derivative operators preserve constraints (2.12). Moreover, (f_u, f_w) are C^1 near the point $(\varphi, 0, 0) \in H^2_u \times \tilde{H}^2_w \times \mathbb{R}$.

To apply the Implicit Function Theorem near this point we require the following criteria:

- (f_u, f_w) must be continuously differentiable.
- $f_u(\varphi, 0, 0) = f_w(\varphi, 0, 0) = 0$
- The Jacobian operator must be invertible at the point $(\varphi, 0, 0)$.

We have already established that (f_u, f_w) are C^1 maps and $(\varphi, 0, 0)$ is a zero of (f_u, f_w).

The Jacobian operator for (2.15) follows from (2.13) and (2.14)

$$\begin{bmatrix} L & 0 \\ 0 & L_0 \end{bmatrix} = \begin{bmatrix} \frac{d^2}{d\tau^2} + \alpha|\varphi|^{\alpha-1} & 0 \\ 0 & \frac{d^2}{d\tau^2} \end{bmatrix} \tag{2.16}$$

We see that the Jacobian is a diagonal operator, with diagonal entries L and L_0 defined in equations (2.6) and (2.7). These both allow one-dimensional kernels in $L^2_{\text{per}}(0, 2\pi)$, but within the constrained spaces H^2_u and $\tilde{H}^2_w$, the kernels are zero-dimensional. This implies that the operators L and L_0 are one-to-one from H^2_u to L^2_u and from $\tilde{H}^2_w$ to $\tilde{L}^2_w$ respectively, and thus the Jacobian operator is invertible.

Therefore, we can invoke the Implicit Function Theorem to conclude that there exists a C^1 continuation of the limiting solution (2.1) with respect to ε as the 2π-periodic solution $(u_*, w_*) \in H^2_u \times \tilde{H}^2_w$ of the system of differential advance-delay equations (1.14) near $\varepsilon = 0$. From the explicit expression (2.11) and the formal expansion (2.3), we can see that $\|w_*\|_{H^2_{\text{per}}} = \mathcal{O}(\varepsilon)$ and $\|u_* - \varphi\|_{H^2_{\text{per}}} = \mathcal{O}(\varepsilon^2)$ as $\varepsilon \to 0$. This completes the proof of Theorem 1.

Chapter 3

Spectral Stability of Periodic Travelling Waves Near $\varepsilon = 0$

3.1 Linearization of Periodic Travelling Waves

In order to analyze stability of the solutions to the dimer chain equations (1.4) near $\varepsilon = 0$, we will linearize the system of nonlinear equations (1.4) at the periodic travelling wave solutions of the form (1.13). As a result, we obtain the linearized dimer equations for small perturbations:

$$\begin{cases} \ddot{u}_{2n-1} = V''(\varepsilon w_*(\tau + 2qn) - u_*(\tau + 2qn))(\varepsilon w_{2n} - u_{2n-1}) \\ \qquad\qquad - V''(u_*(\tau + 2qn) - \varepsilon w_*(\tau + 2qn - 2q))(u_{2n-1} - \varepsilon w_{2n-2}), \\ \ddot{w}_{2n} = \varepsilon V''(u_*(\tau + 2qn + 2q) - \varepsilon w_*(\tau + 2qn))(u_{2n+1} - \varepsilon w_{2n}) \\ \qquad\qquad - \varepsilon V''(\varepsilon w_*(\tau + 2qn) - u_*(\tau + 2qn))(\varepsilon w_{2n} - u_{2n-1}), \end{cases} \tag{3.1}$$

where $n \in \mathbb{Z}$. It is worthwhile to note that V'' is continuous but not continuously differentiable. This fact will complicate the analysis of perturbation results for $\varepsilon > 0$. On the other hand, this complication does not occur for

exact solutions (1.24) and (1.27). For exact solution (1.24) with $q = \frac{\pi}{2}$, the linearized system (3.1) is written explicitly as

$$\begin{cases} \ddot{u}_{2n-1} + \alpha|\varphi|^{\alpha-1}u_{2n-1} = \varepsilon\left(V''(-\varphi)w_{2n} + V''(\varphi)w_{2n-2}\right), \\ \ddot{w}_{2n} + 2\varepsilon^2 V''(-\varphi)w_{2n} = \varepsilon V''(-\varphi)(u_{2n+1} + u_{2n-1}). \end{cases} \tag{3.2}$$

For exact solution (1.27) with $q = 0$ or $q = \pi$, we can write the linearized system (3.1) explicitly as

$$\begin{cases} \ddot{u}_{2n-1} + \frac{\alpha}{1+\varepsilon^2}|\varphi|^{\alpha-1}u_{2n-1} = \frac{\varepsilon}{1+\varepsilon^2}\left(V''(-\varphi)w_{2n} + V''(\varphi)w_{2n-2}\right), \\ \ddot{w}_{2n} + \frac{\alpha\varepsilon^2}{1+\varepsilon^2}|\varphi|^{\alpha-1}w_{2n} = \frac{\varepsilon}{1+\varepsilon^2}\left(V''(\varphi)u_{2n+1} + V''(-\varphi)u_{2n-1}\right). \end{cases} \tag{3.3}$$

In both cases, we can see that the linearized systems (3.2) and (3.3) are analytic in ε near $\varepsilon = 0$.

The system of linearized equations (3.1) has the same symplectic structure (1.10) as the nonlinear system (1.4), but the Hamiltonian is given by

$$\begin{aligned} H &= \frac{1}{2}\sum_{n\in\mathbb{Z}}\left(p_{2n-1}^2 + q_{2n}^2\right) \\ &\quad + \frac{1}{2}\sum_{n\in\mathbb{Z}} V''(\varepsilon w_*(\tau+2qn) - u_*(\tau+2qn))(\varepsilon w_{2n} - u_{2n-1})^2 \\ &\quad + \frac{1}{2}\sum_{n\in\mathbb{Z}} V''(u_*(\tau+2qn) - \varepsilon w_*(\tau+2qn-2q))(u_{2n-1} - \varepsilon w_{2n-2})^2. \end{aligned} \tag{3.4}$$

The Hamiltonian, H, is quadratic in the canonical variables $\{u_{2n-1}, p_{2n-1} = \dot{u}_{2n-1}, w_{2n}, q_{2n} = \dot{w}_{2n}\}_{n\in\mathbb{Z}}$.

3.2 Main Result

The coefficients of the linearized dimer system (3.1) are 2π-periodic in τ. This suggests we look for an infinite-dimensional analogue of the Floquet theorem which states that all solutions of the linear system with 2π-periodic coefficients satisfy the reduction

$$\mathbf{u}(\tau + 2\pi) = \mathcal{M}\mathbf{u}(\tau), \quad \tau \in \mathbb{R}, \tag{3.5}$$

where $\mathbf{u} := [\cdots, w_{2n-2}, u_{2n-1}, w_{2n}, u_{2n+1}, \cdots]$ and $\mathcal{M}$ is the monodromy operator [8].

Remark 4. *We may close the system of dimer equations* (1.4) *into a chain of* $2mN$ *second-order differential equations subject to periodic boundary conditions by setting* $q = \frac{m\pi}{N}$ *as stated in Remark 2. In a similar fashion, we may close the linearized system* (3.1) *as a system of* $2mN$ *second-order linear equations. The monodromy operator,* $\mathcal{M}$ *then becomes an infinite diagonal composition of* $4mN$ *by* $4mN$ *Floquet matrices with* $4mN$ *eigenvalues known as the Floquet multipliers.*

We can find eigenvalues of the monodromy matrix, $\mathcal{M}$ by looking for the set of eigenvectors in the form,

$$u_{2n-1}(\tau) = U_{2n-1}(\tau)e^{\lambda\tau}, \quad u_{2n}(\tau) = W_{2n}(\tau)e^{\lambda\tau}, \quad \tau \in \mathbb{R}, \tag{3.6}$$

where (U_{2n-1}, W_{2n-1}) are 2π-periodic functions and the admissible values of λ are found from the existence of such 2π-periodic functions. The admissible values of λ are known as the *characteristic exponents* and they define the Floquet multipliers, μ, by the formula $\mu = e^{2\pi\lambda}$.

Eigenvectors (3.6) are defined as 2π-periodic solutions of the linear eigenvalue problem,

$$\begin{cases} \ddot{U}_{2n-1} + 2\lambda\dot{U}_{2n-1} + \lambda^2 U_{2n-1} = V''(\varepsilon w_*(\tau+2qn) - u_*(\tau+2qn))(\varepsilon W_{2n} - U_{2n-1}) \\ \qquad\qquad - V''(u_*(\tau+2qn) - \varepsilon w_*(\tau+2qn-2q))(U_{2n-1} - \varepsilon W_{2n-2}), \\ \ddot{W}_{2n} + 2\lambda\dot{W}_{2n} + \lambda^2 W_{2n} = \varepsilon V''(u_*(\tau+2qn+2q) - \varepsilon w_*(\tau+2qn))(U_{2n+1} - \varepsilon W_{2n}) \\ \qquad\qquad - \varepsilon V''(\varepsilon w_*(\tau+2qn) - u_*(\tau+2qn))(\varepsilon W_{2n} - U_{2n-1}). \end{cases} \tag{3.7}$$

This equation is derived from equations (3.1) using the definition (3.6).

The Krein signature plays an important role in the study of spectral stability of periodic solutions [2, Section 4]. The Krein signature is defined as the sign of the 2-form associated with the symplectic structure (1.10):

$$\sigma = i\sum_{n\in\mathbb{Z}} \left[u_{2n-1}\bar{p}_{2n-1} - \bar{u}_{2n-1}p_{2n-1} + w_{2n}\bar{q}_{2n} - \bar{w}_{2n}q_{2n}\right], \tag{3.8}$$

where $\{u_{2n-1}, p_{2n-1} = \dot{u}_{2n-1}, w_{2n}, q_{2n} = \dot{w}_{2n}\}_{n\in\mathbb{Z}}$ is an eigenvector (3.6) associated with an eigenvalue $\lambda \in i\mathbb{R}_+$. It follows from the symmetry of the linearized system (3.1) that if λ is an eigenvalue, then $\bar{\lambda}$ is also an eigenvalue. The 2-form, σ is constant with respect to $\tau \in \mathbb{R}$.

If $\varepsilon = 0$, the monodromy operator, $\mathcal{M}$, in (3.5) is block-diagonal and consists of an infinite set of 2-by-2 Jordan blocks. This occurs because the dimer system (1.4) is decoupled into a countable set of uncoupled second-order differential equations at $\varepsilon = 0$. Therefore, the linear eigenvalue problem (3.7) with the limiting solution (1.19) admits an infinite set of 2π-periodic solutions with $\lambda = 0$,

$$\varepsilon = 0: \quad U^{(0)}_{2n-1} = c_{2n-1}\dot{\varphi}(\tau+2qn), \quad W^{(0)}_{2n} = a_{2n}, \quad n \in \mathbb{Z}, \tag{3.9}$$

where $\{c_{2n-1}, a_{2n}\}_{n\in\mathbb{Z}}$ are arbitrary coefficients. Another countable set of gen-

eralized eigenvectors exists, beyond the eigenvectors (3.9), for the uncoupled second-order differential equations which contribute to the Jordan blocks. Each block corresponds to the double Floquet multiplier $\mu = 1$ (i.e. the double characteristic exponent $\lambda = 0$). When $\varepsilon \neq 0$ but $\varepsilon \ll 1$, the characteristic exponents $\lambda = 0$ of a high multiplicity splits. We study this splitting of characteristic exponents λ by using perturbation arguments.

We formulate the main result of this section.

Theorem 2. *Fix $q = \frac{\pi m}{N}$ for some positive integers m and N such that $1 \leq m \leq N$. Let $(u_*, w_*) \in H^2_u \times \tilde{H}^2_w$ be defined by Theorem 1 for sufficiently small positive ε. Consider the linear eigenvalue problem (3.7) subject to $2mN$-periodic boundary conditions (1.15). There is a $\varepsilon_0 > 0$ such that, for every $\varepsilon \in (0, \varepsilon_0)$, there exists $q_0(\varepsilon) \in \left(0, \frac{\pi}{2}\right)$ such that for all $q \in (0, q_0(\varepsilon))$ and $q \in (\pi - q_0(\varepsilon), \pi]$, no values of λ with $\mathrm{Re}(\lambda) \neq 0$ exist, whereas for $q \in (q_0(\varepsilon), \pi - q_0(\varepsilon))$, there exist some values of λ with $\mathrm{Re}(\lambda) > 0$.*

Remark 5. *By Theorem 2, periodic travelling waves are spectrally stable for $q \in (0, q_0(\varepsilon))$ and $q \in (\pi - q_0(\varepsilon), \pi]$ and unstable for $q \in (q_0(\varepsilon), \pi - q_0(\varepsilon))$. Therefore, the linearized system (3.2) for the exact solution (1.24) with $q = \frac{\pi}{2}$, subject to periodic boundary conditions, is unstable for small $\varepsilon > 0$. Whereas the linearized system (3.3) for exact solution (1.27) with $q = \pi$ subject to periodic boundary conditions is stable for small $\varepsilon > 0$.*

Remark 6. *The result of Theorem 2 is expected to hold for all values of q in $[0, \pi]$, but the spectrum of the linear eigenvalue problem (3.7) for the characteristic exponent λ becomes continuous and connected to zero. An infinite-dimensional analogue of the perturbation theory is required to study eigenvalues of the monodromy operator $\mathcal{M}$ in this case.*

Remark 7. *The case $q = 0$ is degenerate for an application of the perturbation theory. Nevertheless, we show numerically that the linearized system (3.3) for the exact solution (1.27) with $q = 0$ is stable for small $\varepsilon > 0$ and all characteristic exponents are at least double for any $\varepsilon > 0$.*

3.3 Formal Perturbation Expansions

We normally expect splitting of exponents $\lambda = \mathcal{O}(\varepsilon^{1/2})$, since the limiting linear eigenvalue problem at $\varepsilon = 0$ is diagonally decomposed into 2-by-2 Jordan blocks [23]. The splitting we see occurs at a higher order, $\mathcal{O}(\varepsilon)$, since the coupling between the particles of equal masses occurs at $\mathcal{O}(\varepsilon^2)$ in the perturbation theory. Perturbation computations in $\mathcal{O}(\varepsilon^2)$ require V'' to be at least C^1. This creates an obstacle since V'' is only continuous. In our computations we neglect this discrepancy, which is valid at least for $q = \pi$ and $q = \frac{\pi}{2}$. For other values of q, we use a renormalization technique in order to justify the formal perturbation expansion.

We expand 2π-periodic solutions of the linear eigenvalue problem (3.7) in a power series in ε:

$$\lambda = \varepsilon\lambda^{(1)} + \varepsilon^2\lambda^{(2)} + \mathrm{o}(\varepsilon^2) \tag{3.10}$$

and

$$\begin{cases} U_{2n-1} = U_{2n-1}^{(0)} + \varepsilon U_{2n-1}^{(1)} + \varepsilon^2 U_{2n-1}^{(2)} + \mathrm{o}(\varepsilon^2), \\ W_{2n} = W_{2n}^{(0)} + \varepsilon W_{2n}^{(1)} + \varepsilon^2 W_{2n}^{(2)} + \mathrm{o}(\varepsilon^2), \end{cases} \tag{3.11}$$

where the zeroth-order terms are given by (3.9). In order to determine unique

corrections to the power series expansion, we require that

$$\langle \dot{\varphi}, U^{(j)}_{2n-1} \rangle_{L^2_{\text{per}}} = \langle 1, W^{(j)}_{2n} \rangle_{L^2_{\text{per}}} = 0, \quad n \in \mathbb{Z}, \quad j = 1, 2. \tag{3.12}$$

Note that if $U^{(j)}_{2n-1}$ contains a component which is parallel to $\dot{\varphi}$ then the corresponding term will change the value of c_{2n-1} in the eigenvector (3.9). Similarly, if a 2π-periodic function $W^{(j)}_{2n}$ has nonzero mean, then the mean value of $W^{(j)}_{2n}$ will change the value of a_{2n} in eigenvector (3.9). These coefficients are yet to be determined, and thus our condition is justified.

The linear equations (3.7) are satisfied at $\mathcal{O}(\varepsilon^0)$. At $\mathcal{O}(\varepsilon)$, we obtain the equations

$$\begin{cases} \ddot{U}^{(1)}_{2n-1} + \alpha|\varphi(\tau+2qn)|^{\alpha-1}U^{(1)}_{2n-1} = -2\lambda^{(1)}\dot{U}^{(0)}_{2n-1} \\ \qquad\qquad + V''(-\varphi(\tau+2qn))W^{(0)}_{2n} + V''(\varphi(\tau+2qn))W^{(0)}_{2n-2}, \\ \ddot{W}^{(1)}_{2n} = -2\lambda^{(1)}\dot{W}^{(0)}_{2n} + V''(\varphi(\tau+2qn+2q))U^{(0)}_{2n+1} + V''(-\varphi(\tau+2qn))U^{(0)}_{2n-1}. \end{cases} \tag{3.13}$$

Let us define solutions of the following linear inhomogeneous equations:

$$\ddot{v} + \alpha|\varphi|^{\alpha-1}v = -2\ddot{\varphi}, \tag{3.14}$$

$$\ddot{y}_\pm + \alpha|\varphi|^{\alpha-1}y_\pm = V''(\pm\varphi), \tag{3.15}$$

$$\ddot{z}_\pm = V''(\pm\varphi)\dot{\varphi}. \tag{3.16}$$

If we can find unique 2π-periodic solutions of these equations such that

$$\langle \dot{\varphi}, v \rangle_{L^2_{\text{per}}} = \langle \dot{\varphi}, y_\pm \rangle_{L^2_{\text{per}}} = \langle 1, z_\pm \rangle_{L^2_{\text{per}}} = 0,$$

then the perturbation equations (3.13) at the $\mathcal{O}(\varepsilon)$ order are satisfied with

$$\begin{cases} U_{2n-1}^{(1)} = c_{2n-1}\lambda^{(1)}v(\tau+2qn) + a_{2n}y_-(\tau+2qn) + a_{2n-2}y_+(\tau+2qn), \\ W_{2n}^{(1)} = c_{2n+1}z_+(\tau+2qn+2q) + c_{2n-1}z_-(\tau+2qn). \end{cases} \tag{3.17}$$

The linear equations (3.7) are now satisfied up to the $\mathcal{O}(\varepsilon)$ order. Collecting terms at the $\mathcal{O}(\varepsilon^2)$ order, we obtain

$$\begin{cases} \ddot{U}_{2n-1}^{(2)} + \alpha|\varphi(\tau+2qn)|^{\alpha-1}U_{2n-1}^{(2)} = -2\lambda^{(1)}\dot{U}_{2n-1}^{(1)} - 2\lambda^{(2)}\dot{U}_{2n-1}^{(0)} - (\lambda^{(1)})^2U_{2n-1}^{(0)} \\ \qquad + V''(-\varphi(\tau+2qn))W_{2n}^{(1)} + V''(\varphi(\tau+2qn))W_{2n-2}^{(1)} \\ \qquad - V'''(-\varphi(\tau+2qn))(w_*^{(1)}(\tau+2qn) - u_*^{(2)}(\tau+2qn))U_{2n-1}^{(0)} \\ \qquad - V'''(\varphi(\tau+2qn))(u_*^{(2)}(\tau+2qn) - w_*^{(1)}(\tau+2qn-2q))U_{2n-1}^{(0)}, \\ \ddot{W}_{2n}^{(2)} = -2\lambda^{(1)}\dot{W}_{2n}^{(1)} - 2\lambda^{(2)}\dot{W}_{2n}^{(0)} - (\lambda^{(1)})^2W_{2n}^{(0)} \\ \qquad + V''(\varphi(\tau+2qn+2q))(U_{2n+1}^{(1)} - W_{2n}^{(0)}) + V''(-\varphi(\tau+2qn))(U_{2n-1}^{(1)} - W_{2n}^{(0)}), \end{cases} \tag{3.18}$$

where corrections $u_*^{(2)}$ and $w_*^{(1)}$ are defined by expansion (2.3).

To solve the linear inhomogeneous equations (3.18) the source terms must satisfy the Fredholm conditions because the operators L_0 and L defined by (2.6) and (2.7) have one-dimensional kernels. We require the first equation of (3.18) to be orthogonal to $\dot{\varphi}$ and the second equation of system (3.18) to be orthogonal to 1. We substitute (3.9) and (3.17) into the orthogonality conditions (i.e. substitute the solutions into the system (3.18), multiply the first equation by $\dot{\varphi}$ and the second by 1, and integrate on $[-\pi,\pi]$. Taking into account the symmetry between couplings of lattice sites on $\mathbb{Z}$, we obtain difference equations for $\{c_{2n-1}, a_{2n}\}_{n\in\mathbb{Z}}$:

$$\begin{cases} K\Lambda^2 c_{2n-1} = M_1(c_{2n+1} + c_{2n-3} - 2c_{2n-1}) + L_1\Lambda(a_{2n} - a_{2n-2}), \\ \Lambda^2 a_{2n} = M_2(a_{2n+2} + a_{2n-2} - 2a_{2n}) + L_2\Lambda(c_{2n+1} - c_{2n-1}), \end{cases} \tag{3.19}$$

where $\Lambda = \lambda^{(1)}$ and (K, M_1, M_2, L_1, L_2) are numerical coefficients to be com-

puted from the projections. In particular, the coefficients are defined as

$$\begin{aligned}
K &= \int_{-\pi}^{\pi} (2\dot{v}(\tau) + \dot{\varphi}(\tau))\,\dot{\varphi}(\tau) d\tau, \\
M_1 &= \int_{-\pi}^{\pi} V''(-\varphi(\tau))\dot{\varphi}(\tau) z_+(\tau + 2q) d\tau = \int_{-\pi}^{\pi} V''(\varphi(\tau))\dot{\varphi}(\tau) z_-(\tau - 2q) d\tau, \\
M_2 &= \frac{1}{2\pi}\int_{-\pi}^{\pi} V''(\varphi(\tau + 2q)) y_-(\tau + 2q) d\tau = \frac{1}{2\pi}\int_{-\pi}^{\pi} V''(-\varphi(\tau)) y_+(\tau) d\tau, \\
L_1 &= -2\int_{-\pi}^{\pi} \dot{y}_-(\tau)\dot{\varphi}(\tau) d\tau = 2\int_{-\pi}^{\pi} \dot{y}_+(\tau)\dot{\varphi}(\tau) d\tau, \\
L_2 &= \frac{1}{2\pi}\int_{-\pi}^{\pi} V''(\varphi(\tau + 2q)) v(\tau + 2q) d\tau = -\frac{1}{2\pi}\int_{-\pi}^{\pi} V''(-\varphi(\tau)) v(\tau) d\tau.
\end{aligned}$$

It is worth noting that the coefficients M_1 and M_2 need not be computed at the diagonal terms c_{2n-1} and a_{2n} due to the fact that the difference equations (3.19) with $\Lambda = 0$ must have eigenvectors with equal values of $\{c_{2n-1}\}_{n\in\mathbb{Z}}$ and $\{a_{2n}\}_{n\in\mathbb{Z}}$ which correspond to the two symmetries of the linearized dimer system (3.1) related to symmetries (1.7) and (1.8). This fact suggests that the problem of limited smoothness of V'', which is C but not C^1 near zero, is not a serious obstacle in the derivation of the reduced system (3.19).

Difference equations (3.19) give a necessary and sufficient condition to solve the linear inhomogeneous equations (3.18) at $\mathcal{O}(\varepsilon^2)$ and continue the perturbation expansions beyond this order.

The system of difference equations (3.19) presents a quadratic eigenvalue problem with respect to the spectral parameter Λ. Such quadratic eigenvalue problems often appear in the context of spectral stability of nonlinear waves [5, 19].

Before justifying the formal perturbation expansions, we shall explicitly compute the coefficients (K, M_1, M_2, L_1, L_2) of the difference equations (3.19).

3.4 Computation of Coefficients

We prove the following technical result.

Lemma 1. *Coefficients K, M_2, L_1, and L_2 are independent of q and are given by*

$$K = -\frac{4\pi^2}{T'(E_0)}, \quad M_2 = \frac{2}{\pi T'(E_0)(\dot{\varphi}(0))^2}, \quad L_1 = 2\pi L_2 = \frac{2(2\pi - T'(E_0)(\dot{\varphi}(0))^2)}{T'(E_0)\dot{\varphi}(0)}.$$

Consequently, $K > 0$, whereas $M_2, L_1, L_2 < 0$. On the other hand, coefficient M_1 depends on q and is given by

$$M_1 = -\frac{2}{\pi}(\dot{\varphi}(0))^2 + I(q),$$

where

$$I(q) = I(\pi - q) := -\int_{\pi-2q}^{\pi} \ddot{\varphi}(\tau)\ddot{\varphi}(\tau + 2q)d\tau, \quad q \in \left[0, \frac{\pi}{2}\right].$$

To prove Lemma 1, we must first find unique solutions to the linear inhomogeneous equations (3.14), (3.15) and (3.16). For equation (3.14), the general solution is given by

$$v(\tau) = -\tau\dot{\varphi}(\tau) + b_1\dot{\varphi}(\tau) + b_2\partial_E\varphi_{E_0}(\tau), \quad \tau \in [-\pi, \pi],$$

where (b_1, b_2) are arbitrary coefficients and $\partial_E\varphi_{E_0}$ is the derivative of the $T(E)$-periodic solution φ_E of the nonlinear oscillator equation (1.17) with first integral (1.18) satisfying initial conditions $\varphi_E(0) = 0$ and $\dot{\varphi}_E(0) = \sqrt{2E}$ at energy

$E = E_0$, for which $T(E_0) = 2\pi$. We note the equation

$$\partial_E \varphi_{E_0}(\pm\pi) = \mp\frac{1}{2}T'(E_0)\dot{\varphi}(\pm\pi), \tag{3.20}$$

follows from differentiation of equation $\varphi_E(\pm T(E)/2) = 0$ with respect to E at $E = E_0$.

To define v uniquely, we require that $\langle \dot{\varphi}, v\rangle_{L^2_{\text{per}}} = 0$. This condition along with the fact that $\tau\dot{\varphi}$ and $\partial_E\varphi_{E_0}$ are odd and $\dot{\varphi}$ is even in τ force $b_1 = 0$ and thus $v(0) = 0$. Therefore, v is odd in τ. In order to satisfy the 2π-periodicity, we require $v(\pi) = 0$, which will uniquely determine b_2 by virtue of (3.20) as

$$b_2 = \frac{\pi\dot{\varphi}(\pi)}{\partial_E\varphi_{E_0}(\pi)} = -\frac{2\pi}{T'(E_0)}.$$

We have now uniquely determined $v(\tau)$ as

$$v(\tau) = -\tau\dot{\varphi}(\tau) - \frac{2\pi}{T'(E_0)}\partial_E\varphi_{E_0}(\tau), \quad \tau \in [-\pi, \pi]. \tag{3.21}$$

For equation (3.15), we take advantage of the fact that $\varphi(\tau) \geq 0$ for $\tau \in [0, \pi]$ and $\varphi(\tau) \leq 0$ for $\tau \in [-\pi, 0]$. We also use the symmetry $\dot{\varphi}(\pi) = -\dot{\varphi}(0)$. Integrating the equations for $y_\pm$ separately from equation (3.15), we obtain solutions

$$y_+(\tau) = \begin{cases} 1 + a_+\dot{\varphi} + b_+\partial_E\varphi_{E_0}, & \tau \in [-\pi, 0], \\ c_+\dot{\varphi} + d_+\partial_E\varphi_{E_0}, & \tau \in [0, \pi], \end{cases}$$

$$y_-(\tau) = \begin{cases} a_-\dot{\varphi} + b_-\partial_E\varphi_{E_0}, & \tau \in [-\pi, 0], \\ 1 + c_-\dot{\varphi} + d_-\partial_E\varphi_{E_0}, & \tau \in [0, \pi]. \end{cases}$$

We use continuity of $y_\pm$ and $\dot{y}_\pm$ across $\tau = 0$ to uniquely determine $d_\pm = b_\pm$

and $c_\pm = a_\pm \pm \frac{1}{\dot\varphi(0)}$. The solutions are 2π-periodic if $y_\pm(-\pi) = y_\pm(\pi)$, which gives

$$b_\pm = \pm \frac{2}{T'(E_0)\dot\varphi(0)}.$$

We note that the constants $a_\pm$ are still unspecified.

In order to define $y_\pm$ uniquely, we require orthogonality $\langle \dot\varphi, y_\pm \rangle_{L^2_{\rm per}} = 0$. This forces the constraints on $a_\pm$,

$$a_\pm = \mp \frac{1}{2\dot\varphi(0)} \mp \frac{2\langle \dot\varphi, \partial_E \varphi_{E_0} \rangle_{L^2_{\rm per}}}{T'(E_0)\dot\varphi(0)\langle \dot\varphi, \dot\varphi \rangle_{L^2_{\rm per}}}.$$

Thus, we obtain a unique solution for $y_\pm$,

$$y_+(\tau) = a_+\dot\varphi(\tau) + b_+\partial_E\varphi_{E_0}(\tau) + \begin{cases} 1, & \tau \in [-\pi, 0], \\ \frac{\dot\varphi(\tau)}{\dot\varphi(0)}, & \tau \in [0, \pi], \end{cases} \tag{3.22}$$

and

$$y_-(\tau) = a_-\dot\varphi(\tau) + b_-\partial_E\varphi_{E_0}(\tau) + \begin{cases} 0, & \tau \in [-\pi, 0], \\ 1 - \frac{\dot\varphi(\tau)}{\dot\varphi(0)}, & \tau \in [0, \pi], \end{cases} \tag{3.23}$$

where $(a_\pm, b_\pm)$ are uniquely defined as above.

Equation (3.16) can be integrated separately on $[-\pi, 0]$ and $[0, \pi]$ to obtain

$$\dot z_+(\tau) = \begin{cases} c_+ - |\varphi(\tau)|^\alpha, & \tau \in [-\pi, 0], \\ c_+, & \tau \in [0, \pi], \end{cases}$$

$$\dot z_-(\tau) = \begin{cases} c_-, & \tau \in [-\pi, 0], \\ c_- + |\varphi(\tau)|^\alpha, & \tau \in [0, \pi], \end{cases}$$

where (c_+, c_-) are constants of integration and continuity of $\dot z_\pm$ across $\tau = 0$

has been used. Again, we require $\langle 1, z_\pm \rangle_{L^2_{\rm per}} = 0$ in order to uniquely define $z_\pm$. Integrating the above equation once under this condition, we find:

$$z_+(\tau) = \begin{cases} c_+\tau + d_+ - \dot\varphi(\tau), & \tau \in [-\pi, 0], \\ c_+\tau - d_+, & \tau \in [0, \pi], \end{cases}$$
$$z_-(\tau) = \begin{cases} c_-\tau + d_-, & \tau \in [-\pi, 0], \\ c_-\tau - d_- - \dot\varphi(\tau), & \tau \in [0, \pi], \end{cases}$$

where (d_+, d_-) are constants of integration. Continuity of $z_\pm$ across $\tau = 0$ sets the coefficient $d_\pm = \pm\frac{1}{2}\dot\varphi(0)$. Periodicity of $z_\pm(-\pi) = z_\pm(\pi)$ defines the coefficient $c_\pm = \pm\frac{1}{\pi}\dot\varphi(0)$. Therefore we can write a unique solution to equation (3.16) as

$$z_+(\tau) = \frac{1}{2\pi} \begin{cases} \dot\varphi(0)(2\tau + \pi) - 2\pi\dot\varphi(\tau), & \tau \in [-\pi, 0], \\ \dot\varphi(0)(2\tau - \pi), & \tau \in [0, \pi], \end{cases} \tag{3.24}$$

and

$$z_-(\tau) = \frac{1}{2\pi} \begin{cases} -\dot\varphi(0)(2\tau + \pi), & \tau \in [-\pi, 0], \\ -\dot\varphi(0)(2\tau - \pi) - 2\pi\dot\varphi(\tau), & \tau \in [0, \pi]. \end{cases} \tag{3.25}$$

Using solutions (3.21), (3.22), (3.23), (3.24) and (3.25) we can now compute the coefficients (K, M_1, M_2, L_1, L_2) of the difference equations (3.19). For K, we integrate by parts and use equations (1.17), (1.18) and (3.21) to obtain

$$\begin{aligned} K &= \int_{-\pi}^{\pi} \dot\varphi(\dot\varphi + 2\dot v) d\tau = \int_{-\pi}^{\pi} (\dot\varphi^2 - 2v\ddot\varphi) d\tau \\ &= \left[\tau\dot\varphi^2 + \frac{2\pi}{T'(E_0)}\partial_E\varphi_{E_0}\dot\varphi\right]\Big|_{\tau=-\pi}^{\tau=\pi} + \frac{2\pi}{T'(E_0)}\int_{-\pi}^{\pi} (\partial_E\varphi_{E_0}\ddot\varphi - \partial_E\dot\varphi_{E_0}\dot\varphi)\, d\tau \\ &= -\frac{4\pi}{T'(E_0)}\int_0^{\pi} \partial_E\left(\frac{1}{2}\dot\varphi^2 + \frac{1}{1+\alpha}\varphi^{1+\alpha}\right)_{E_0} d\tau = -\frac{4\pi^2}{T'(E_0)}. \end{aligned}$$

As stated in Section 1.3, $T'(E_0) < 0$ and so $K > 0$.

For M_1, we use equations (3.16), (3.24), and (3.25) to obtain

$$\begin{aligned} M_1 &= \int_{-\pi}^{\pi} V''(-\varphi(\tau))\dot{\varphi}(\tau) z_+(\tau + 2q)d\tau = \int_{-\pi}^{\pi} \ddot{z}_-(\tau) z_+(\tau + 2q)d\tau \\ &= -\int_{-\pi}^{\pi} \dot{z}_-(\tau)\dot{z}_+(\tau + 2q)d\tau = \int_0^{\pi} \ddot{\varphi}(\tau)\dot{z}_+(\tau + 2q)d\tau. \end{aligned}$$

Note that the sign of M_1 depends on q. Using solution (3.25), for $q \in \left[0, \frac{\pi}{2}\right]$, we obtain

$$\begin{aligned} M_1 &= \frac{1}{\pi}\dot{\varphi}(0)\int_0^{\pi} \ddot{\varphi}(\tau)d\tau - \int_{\pi-2q}^{\pi} \ddot{\varphi}(\tau)\ddot{\varphi}(\tau + 2q)d\tau \\ &= -\frac{2}{\pi}(\dot{\varphi}(0))^2 + I(q), \quad I(q) := -\int_{\pi-2q}^{\pi} \ddot{\varphi}(\tau)\ddot{\varphi}(\tau + 2q)d\tau. \end{aligned}$$

For $q \in \left[\frac{\pi}{2}, \pi\right]$, we obtain

$$M_1 = -\frac{2}{\pi}(\dot{\varphi}(0))^2 + \tilde{I}(q), \quad \tilde{I}(q) := -\int_0^{2\pi-2q} \ddot{\varphi}(\tau)\ddot{\varphi}(\tau + 2q)d\tau,$$

and

$$\tilde{I}(\pi - q) = -\int_0^{2q} \ddot{\varphi}(\tau)\ddot{\varphi}(\tau - 2q)d\tau = -\int_{-2q}^{0} \ddot{\varphi}(\tau)\ddot{\varphi}(\tau + 2q)d\tau = I(q),$$

since the mean value of a periodic function does not depend on the limits of integration.

For M_2, we use equations (3.15) and (3.22):

$$\begin{aligned} M_2 &= \frac{1}{2\pi}\int_{-\pi}^{\pi} V''(-\varphi) y_+ d\tau = \frac{\alpha}{2\pi}\int_0^{\pi} \varphi^{\alpha-1} y_+ d\tau \\ &= -\frac{1}{2\pi}\int_0^{\pi} \ddot{y}_+ d\tau = \frac{1}{\pi} b_+ \partial_E \dot{\phi}_{E_0}(0) = \frac{2}{\pi T'(E_0)(\dot{\varphi}(0))^2}, \end{aligned}$$

and, again since $T'(E_0) < 0$, we have $M_2 < 0$.

For L_1, we may use (1.17), (1.18) and (3.23) to find

$$\begin{aligned} L_1 &= -2\int_{-\pi}^{\pi} \dot{y}_- \dot{\varphi} d\tau = -2b_- \int_{-\pi}^{\pi} \partial_E \dot{\varphi}_{E_0} \dot{\varphi} d\tau \\ &= \frac{4}{T'(E_0)\dot{\varphi}(0)} \left[\int_0^{\pi} \left(\partial_E \dot{\varphi}_{E_0} \dot{\varphi} - \partial_E \varphi_{E_0} \ddot{\varphi} \right) d\tau + \dot{\varphi} \partial_E \varphi_{E_0} \Big|_{\tau=0}^{\tau=\pi} \right] \\ &= \frac{2(2\pi - T'(E_0)(\dot{\varphi}(0))^2)}{T'(E_0)\dot{\varphi}(0)}. \end{aligned}$$

By construction $\dot{\varphi}(0) > 0$, and since $T'(E_0) < 0$ we have $L_1 < 0$.

For L_2, we can use (1.17), (1.18) and (3.21) to get

$$\begin{aligned} L_2 &= -\frac{1}{2\pi} \int_{-\pi}^{\pi} V''(-\varphi) v d\tau = -\frac{\alpha}{2\pi} \int_0^{\pi} \varphi^{\alpha-1} v d\tau \\ &= \frac{1}{T'(E_0)} \int_0^{\pi} \partial_E \left(\varphi_{E_0} \right)^{\alpha} d\tau - \frac{1}{2\pi} \int_0^{\pi} \varphi^{\alpha} d\tau \\ &= \left[\frac{1}{2\pi} \dot{\varphi} - \frac{1}{T'(E_0)} \partial_E \dot{\varphi}_{E_0} \right] \Big|_{\tau=0}^{\tau=\pi} \\ &= \frac{2\pi - T'(E_0)(\dot{\varphi}(0))^2}{\pi T'(E_0)\dot{\varphi}(0)} = \frac{1}{2\pi} L_1, \end{aligned}$$

and hence $L_2 < 0$.

This completes the proof of Lemma 1.

3.5 Eigenvalues of Difference Equations

The coefficients (K, M_1, M_2, L_1, L_2) of difference equations (3.19) are independent of n. This means we can solve these equations by means of a discrete Fourier transform. We make the substitution

$$c_{2n-1} = Ce^{i\theta(2n-1)}, \quad a_{2n} = Ae^{i2\theta n}, \tag{3.26}$$

where $\theta \in [0, \pi]$ is the Fourier spectral parameter. With this substitution, we obtain the system of linear homogeneous equations from the difference equations (3.19):

$$\begin{cases} K\Lambda^2 C = 2M_1(\cos(2\theta) - 1)C + 2iL_1\Lambda\sin(\theta)A, \\ \Lambda^2 A = 2M_2(\cos(2\theta) - 1)A + 2iL_2\Lambda\sin(\theta)C. \end{cases} \tag{3.27}$$

A nonzero solution of system (3.27) exists if and only if Λ is a root of the characteristic polynomial

$$D(\Lambda;\theta) = K\Lambda^4 + 4\Lambda^2(M_1 + KM_2 + L_1L_2)\sin^2(\theta) + 16M_1M_2\sin^4(\theta) = 0. \tag{3.28}$$

This equation is bi-quadratic and thus has two pairs of roots for each $\theta \in [0, \pi]$. For $\theta = 0$, both pairs are identically zero. This recovers the characteristic exponent, $\lambda = 0$ of algebraic multiplicity of at least 4 in the linear eigenvalue problem (3.7). For a fixed $\theta \in (0, \pi)$, the two pairs of roots are generally nonzero and given by Λ_1^2 and Λ_2^2. The following lemma specifies their location.

Lemma 2. *There exists a* $q_0 \in \left(0, \frac{\pi}{2}\right)$ *such that* $\Lambda_1^2 \leq \Lambda_2^2 < 0$ *for* $q \in [0, q_0) \cup (\pi - q_0, \pi]$ *and* $\Lambda_1^2 < 0 < \Lambda_2^2$ *for* $q \in (q_0, \pi - q_0)$.

To classify the nonzero roots of the characteristic polynomial (3.28), we define

$$\Gamma := M_1 + KM_2 + L_1L_2, \quad \Delta := 4KM_1M_2. \tag{3.29}$$

The two pairs of roots are determined in the following table.

Coefficients	Roots
$\Delta < 0$	$\Lambda_1^2 < 0 < \Lambda_2^2$
$0 < \Delta \leq \Gamma^2$, $\Gamma > 0$	$\Lambda_1^2 \leq \Lambda_2^2 < 0$
$0 < \Delta \leq \Gamma^2$, $\Gamma < 0$	$0 < \Lambda_1^2 \leq \Lambda_2^2$
$\Delta > \Gamma^2$	$\mathrm{Re}(\Lambda_1^2) > 0,\ \mathrm{Re}(\Lambda_2^2) < 0$

Table 4.1: Squared roots of the characteristic equation (3.28).

Substituting the explicit computations of coefficients (K, M_1, M_2, L_1, L_2) found in Section 3.4, we obtain

$$\Gamma = -\frac{8}{T'(E_0)} + I(q),$$
$$\Delta = \frac{64}{(T'(E_0))^2}\left(1 - \frac{\pi I(q)}{2(\dot{\varphi}(0))^2}\right).$$

The function $I(q)$ is symmetric about $q = \frac{\pi}{2}$ as shown in Lemma 1. Therefore, we may restrict our consideration to the values $q \in \left[0, \frac{\pi}{2}\right]$ and use the explicit definition of $I(q)$:

$$I(q) = -\int_{\pi-2q}^{\pi} \ddot{\varphi}(\tau)\ddot{\varphi}(\tau + 2q)d\tau, \quad q \in \left[0, \frac{\pi}{2}\right].$$

It is clear that $I(0) = 0$. We can show that $I(q)$ is a monotonically increasing function in $\left[0, \frac{\pi}{2}\right]$.

Firstly, by (1.17), $\ddot{\varphi}(\tau) = -|\varphi(\tau)|^{\alpha-1}\varphi(\tau)$. Since $\varphi(\tau) \geq 0$ on $\tau \in [0, \pi]$, we have that $\ddot{\varphi}(\tau) \leq 0$ on $\tau \in [0, \pi]$. As well, $\ddot{\varphi}(\tau + 2q) \geq 0$ for $\tau \in [\pi - 2q, \pi]$. We then have $I(q) \geq 0$ for $2q \in [0.\pi]$. Moreover, we can show that I is a C^1

function of q, because the first derivative, given by,

$$\begin{aligned} I'(q) &= -2\int_{\pi-2q}^{\pi} \ddot{\varphi}(\tau)\dddot{\varphi}(\tau+2q)d\tau = 2\int_{\pi-2q}^{\pi} \dddot{\varphi}(\tau)\ddot{\varphi}(\tau+2q)d\tau \\ &= -2\alpha\int_{\pi-2q}^{\pi} |\varphi(\tau)|^{\alpha-1}\dot{\varphi}(\tau)\ddot{\varphi}(\tau+2q)d\tau, \end{aligned}$$

is continuous for all $2q \in [0,\pi]$. The functions $\dot{\varphi}(\tau)$ and $\ddot{\varphi}(\tau)$ are odd and even, respectively, with respect to $\tau = \frac{\pi}{2}$. We have already established that $\ddot{\varphi}(\tau+2q) \geq 0$ on $\tau \in [\pi-2q,\pi]$. We also have that $\dot{\varphi}(\tau) \geq 0$ on $\tau \in \left[0,\frac{\pi}{2}\right]$ and $\dot{\varphi}(\tau) \leq 0$ on $\tau \in \left[\frac{\pi}{2},\pi\right]$. Thus, $I'(q) \geq 0$ for all $2q \in [0,\pi]$. Therefore, $I(q)$ is monotonically increasing from $I(0) = 0$ to

$$I\left(\frac{\pi}{2}\right) = -\int_0^{\pi} \ddot{\varphi}(\tau)\ddot{\varphi}(\tau+\pi)d\tau = \int_0^{\pi} (\ddot{\varphi}(\tau))^2 d\tau > 0.$$

Hence, for all $q \in \left[0,\frac{\pi}{2}\right]$ we have $\Gamma > 0$ and

$$\Gamma^2 - \Delta = I(q)\left(I(q) - \frac{16}{T'(E_0)} + \frac{32\pi}{(T'(E_0)\dot{\varphi}(0))^2}\right) \geq 0,$$

where $\Delta = \Gamma^2$ if and only if $q = 0$. We see that only the first two lines of Table 4.1 can occur.

For $q = 0$, $I(0) = 0$ hence $M_1 < 0$, $\Delta > 0$ and $\Delta = \Gamma^2$. The second line of Table 4.1 gives $\Lambda_1^2 = \Lambda_2^2 < 0$. All characteristic exponents are purely imaginary and degenerate, thanks to the explicit computations:

$$\Lambda_1^2 = \Lambda_2^2 = -\frac{4}{\pi^2}\sin^2(\theta). \tag{3.30}$$

The proof of Lemma 2 is complete if we can show that there is a $q_0 \in \left(0,\frac{\pi}{2}\right)$ such that the first line of Table 4.1 yields $\Lambda_1^2 < 0 < \Lambda_2^2$ for $q \in \left(q_0,\frac{\pi}{2}\right]$

and the second line of Table 4.1 yields $\Lambda_1^2 < \Lambda_2^2 < 0$ for $q \in (0, q_0)$. Because I is monotonically increasing as a function of q and $\Delta > 0$ for $q = 0$ the existence of $q_0 \in \left(0, \frac{\pi}{2}\right)$ follows by continuity if $\Delta < 0$ for $q = \frac{\pi}{2}$. Since $K > 0$ and $M_2 < 0$, we need to prove that $M_1 > 0$ for $q = \frac{\pi}{2}$. Equivalently,

$$I\left(\frac{\pi}{2}\right) > \frac{2}{\pi}\left(\dot{\varphi}(0)\right)^2.$$

Since $\dot{\varphi}$ is a 2π-periodic function with zero mean, the Poincaré inequality yields

$$I\left(\frac{\pi}{2}\right) = \frac{1}{2}\int_{-\pi}^{\pi}(\ddot{\varphi}(\tau))^2 d\tau \geq \frac{1}{2}\int_{-\pi}^{\pi}(\dot{\varphi}(\tau))^2 d\tau.$$

Using (1.17) and (1.18) along with integration by parts we see

$$\frac{1}{2}\int_{-\pi}^{\pi}(\dot{\varphi}(\tau))^2 d\tau = -\frac{1}{2}\int_{-\pi}^{\pi}\varphi(\tau)\ddot{\varphi}(\tau)d\tau = \frac{1}{2}\int_{-\pi}^{\pi}|\varphi(\tau)|^{\alpha+1}d\tau = \frac{2\pi(\alpha+1)}{(\alpha+3)}E.$$

The last equality comes from integrating the invariant (1.18) on $[-\pi, \pi]$. Therefore, we obtain

$$I\left(\frac{\pi}{2}\right) \geq \frac{2\pi(\alpha+1)}{(\alpha+3)}E = \frac{\pi(\alpha+1)}{(\alpha+3)}(\dot{\varphi}(0))^2 > \frac{2}{\pi}(\dot{\varphi}(0))^2,$$

where the final inequality holds for $\alpha = \frac{3}{2}$ based on the fact that $\frac{5\pi^2}{18} \approx 2.74 > 1$. Therefore $M_1 > 0$ and as a result $\Delta < 0$ for $q = \frac{\pi}{2}$. This completes the proof of Lemma 2.

Numerical approximations of coefficients Γ and Δ versus q were computed and are shown in Figure 3.1. We can see from the figure that the sign change of Δ occurs at $q_0 \approx 0.915$.

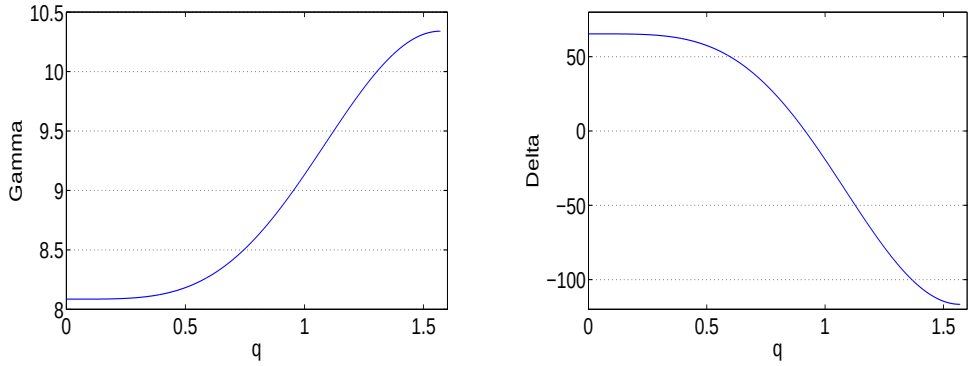

Figure 3.1: Coefficients Γ (left) and Δ (right) versus q.

3.6 Krein Signature of Eigenvalues

Because the eigenvalue problem (3.27) is symmetric with respect to reflection of θ about $\frac{\pi}{2}$, that is, $\sin(\theta) = \sin(\pi - \theta)$, some roots $\Lambda \in \mathbb{C}$ of the characteristic polynomial (3.28) produce multiple eigenvalues λ in the linear eigenvalue problem (3.7) at the $\mathcal{O}(\epsilon)$ order of the asymptotic expansion (3.10). To control splitting and persistence of eigenvalues $\lambda \in i\mathbb{R}_+$ with respect to perturbations, we shall look at the Krein signature of the 2-form σ defined by (3.8). The following result allows us to compute σ asymptotically as $\epsilon \to 0$.

Lemma 3. *For every $q \in (0, q_0)$, the 2-form σ for every eigenvector of the linear eigenvalue problem (3.7) generated by the perturbation expansion (3.11) associated with the root $\Lambda \in i\mathbb{R}_+$ of the characteristic equation (3.28) is nonzero.*

Using the representation (3.6) for $\lambda = i\omega$ with $\omega \in \mathbb{R}_+$, we rewrite σ in the form:

$$\sigma = 2\omega \sum_{n\in\mathbb{Z}} \left[|U_{2n-1}|^2 + |W_{2n}|^2\right] + i \sum_{n\in\mathbb{Z}} \left[U_{2n-1}\dot{\bar{U}}_{2n-1} - \bar{U}_{2n-1}\dot{U}_{2n-1} + W_{2n}\dot{\bar{W}}_{2n} - \bar{W}_{2n}\dot{W}_{2n}\right].$$

Now using perturbation expansion $\omega = \epsilon\Omega + \mathcal{O}(\epsilon^2)$, where $\Lambda = i\Omega \in i\mathbb{R}_+$ is a root of the characteristic equation (3.28), and the perturbation expansions (3.11) for the eigenvector, we compute

$$\sigma = \epsilon \sum_{n\in\mathbb{Z}} \sigma_n^{(1)} + \mathcal{O}(\epsilon^2),$$

where

$$\begin{aligned}\sigma_n^{(1)} &= 2\Omega\left[|c_{2n-1}|^2\dot\varphi^2(\tau+2qn) + |a_{2n}|^2\right] + i(c_{2n-1}\dot{\bar U}_{2n-1}^{(1)} - \bar c_{2n-1}\dot U_{2n-1}^{(1)})\dot\varphi(\tau+2qn)\\ &\quad -i(c_{2n-1}\bar U_{2n-1}^{(1)} - \bar c_{2n-1}U_{2n-1}^{(1)})\ddot\varphi(\tau+2qn) + i(a_{2n}\dot{\bar W}_{2n}^{(1)} - \bar a_{2n}\dot W_{2n}^{(1)}).\end{aligned}$$

Using representation (3.17), this becomes

$$\sigma_n^{(1)} = 2\Omega(|c_{2n-1}|^2E_0 + |a_{2n}|^2) + i(c_{2n-1}\bar a_{2n} - \bar c_{2n-1}a_{2n})E_- + i(c_{2n-1}\bar a_{2n-2} - \bar c_{2n-1}a_{2n-2})E_+,$$

where E_0 and $E_\pm$ are numerical coefficients given by

$$\begin{aligned}E_0 &= \dot\varphi^2 + \dot\varphi\dot v - \ddot\varphi v,\\ E_\pm &= \dot\varphi\dot y_\pm - \ddot\varphi y_\pm - \dot z_\pm.\end{aligned}$$

Using explicit computations of functions v, $y_\pm$, and $z_\pm$ in Section 3.4, we obtain

$$E_0 = -\frac{2\pi}{T'(E_0)}, \quad E_\pm = \pm\frac{2\pi - T'(E_0)(\dot\varphi(0))^2}{\pi T'(E_0)\dot\varphi(0)},$$

and hence we have

$$\sigma_n^{(1)} = 2\Omega\left(\frac{K}{2\pi}|c_{2n-1}|^2 + |a_{2n}|^2\right) - iL_2(c_{2n-1}\bar a_{2n} - \bar c_{2n-1}a_{2n} - c_{2n-1}\bar a_{2n-2} + \bar c_{2n-1}a_{2n-2}).$$

Substituting the eigenvector of the reduced eigenvalue problem (3.19)

in the discrete Fourier transform form (3.26), we obtain

$$\begin{aligned}\sigma_n^{(1)} &= 2\Omega\left(\frac{K}{2\pi}C^2 + A^2\right) - 4L_2\sin(\theta)CA \\ &= \frac{1}{\pi\Omega}\left(\Omega^2 KC^2 + 8\pi M_2\sin^2(\theta)A^2\right),\end{aligned}$$

where the second equation of system (3.27) has been used. Using the first equation of system (3.27), we obtain

$$\sigma_n^{(1)} = \frac{C^2}{\pi L_1 L_2 \Omega^3}\left[KL_1L_2\Omega^4 + M_2(K\Omega^2 - 4M_1\sin^2(\theta))^2\right]. \tag{3.31}$$

Note that $\sigma_n^{(1)}$ is independent of n, hence periodic boundary conditions are used to obtain a finite expression for the 2-form σ.

We consider $q \in (0, q_0)$ and $\theta \in (0, \pi)$, so that $\Omega \neq 0$ and $C \neq 0$. Then, $\sigma_n^{(1)} = 0$ if and only if

$$KL_1L_2\Omega^4 + M_2(K\Omega^2 - 4M_1\sin^2(\theta))^2 = 0.$$

Using the explicit coefficients in Lemma 1, we factorize the left hand side as follows:

$$\begin{aligned}KL_1L_2\Omega^4 + M_2(K\Omega^2 - 4M_1\sin^2(\theta))^2 &= \left(\Omega^2 + T'(E_0)M_1M_2\sin^2(\theta)\right) \\ &\times\left(\frac{32\pi^2}{(T'(E_0))^2}\left(1 - \frac{T'(E_0)(\dot\varphi(0))^2}{4\pi}\right)\Omega^2 + \frac{16}{T'(E_0)}M_1\sin^2(\theta)\right).\end{aligned} \tag{3.32}$$

For every $q \in (0, q_0)$, $M_1 < 0$, so that the second bracket is strictly positive (recall that $T'(E_0) < 0$). Now the first bracket vanishes at

$$\Omega^2 = \frac{-2M_1}{\pi(\dot\varphi(0))^2}\sin^2(\theta).$$

Substituting this constraint to the characteristic equation (3.28) yields after straightforward computations:

$$D(i\Omega;\theta) = \frac{8M_1 \sin^4(\theta)}{\pi\dot{\varphi}^2(0)} \left(1 - \frac{2\pi}{T'(E_0)\dot{\varphi}^2(0)}\right) I(q),$$

which is nonzero for all $q \in (0, q_0)$ and $\theta \in (0, \pi)$. Therefore, $\sigma_n^{(1)}$ does not vanish if $q \in (0, q_0)$ and $\theta \in (0, \pi)$. By continuity of the perturbation expansions in ϵ, σ also does not vanish. The proof of Lemma 3 is complete.

Remark 8. *For every $q \in (0, q_0)$, all roots $\Lambda \in i\mathbb{R}_+$ of the characteristic equation (3.28) are divided into two equal sets, one has $\sigma_n^{(1)} > 0$ and the other one has $\sigma_n^{(1)} < 0$. This follows from the factorization*

$$D(i\Omega;\theta) = -\frac{4\pi^2}{T'(E_0)} \left(\Omega^2 - \frac{4}{\pi^2}\sin^2(\theta)\right)^2 - 4I(q) \left(\Omega^2 - \frac{8}{\pi T'(E_0)(\dot{\varphi}(0))^2}\sin^2(\theta)\right) \sin^2(\theta).$$

As $q \to 0$, $I(q) \to 0$ and perturbation theory for double roots (3.30) *for $q = 0$ yields*

$$\Omega^2 = \frac{4}{\pi^2}\sin^2(\theta) \pm \frac{2}{\pi^2}\sin^2(\theta)\sqrt{|T'(E_0)|I(q)\left(1 - \frac{2\pi}{T'(E_0)(\dot{\varphi}(0))^2}\right)} + \mathcal{O}(I(q)).$$

Using the factorization formula (3.32), the sign of $\sigma_n^{(1)}$ is determined by the expression

$$\Omega^2 + T'(E_0)M_1M_2\sin^2(\theta) = \pm\frac{2}{\pi^2}\sin^2(\theta)\sqrt{|T'(E_0)|I(q)\left(1 - \frac{2\pi}{T'(E_0)(\dot{\varphi}(0))^2}\right)} + \mathcal{O}(I(q)),$$

which justifies the claim for small positive q. By Lemma 3, the Krein signature of $\sigma_n^{(1)}$ does not vanish for all $q \in (0, q_0)$ and $\theta \in (0, \pi)$, therefore the splitting of all roots $\Lambda \in i\mathbb{R}_+$ into two equal sets persists for all values of $q \in (0, q_0)$.

3.7 Proof of Theorem 2

To conclude the proof of Theorem 2, we develop rigorous perturbation theory in the case when $q = \frac{\pi m}{N}$ for some positive integers m and N such that $1 \leq m \leq N$. In this case, the linear eigenvalue problem (3.7) can be closed at $2mN$ second-order differential equations subject to $2mN$-periodic boundary conditions (1.15) and we are looking for $4mN$ eigenvalues λ, which are characteristic values of a $4mN \times 4mN$ Floquet matrix.

At $\varepsilon = 0$, we have $2mN$ double Jordan blocks for $\lambda = 0$. The $2mN$ eigenvectors are given by (3.9). The $2mN$-periodic boundary conditions are incorporated in the discrete Fourier transform (3.26) if

$$\theta = \frac{\pi k}{mN} \equiv \theta_k(m, N), \quad k = 0, 1, \ldots, mN - 1.$$

Because the characteristic equation (3.28) for each $\theta_k(m, N)$ returns 4 roots, we count $4mN$ roots of the characteristic equation (3.28), as many as there are eigenvalues λ in the linear eigenvalue problem (3.7). As long as the roots are non-degenerate (if $\Delta \neq \Gamma^2$) and different from zero (if $\Delta \neq 0$), the first-order perturbation theory predicts splitting of $\lambda = 0$ into symmetric pairs of non-zero eigenvalues. The zero eigenvalue of multiplicity 4 persists and corresponds to the value $\theta_0(m, N) = 0$. It is associated with the symmetries (1.7) and (1.8) of the dimer equations (1.4)

The non-zero eigenvalues are located hierarchically with respect to the values of $\sin^2(\theta)$ for $\theta = \theta_k(m, N)$ with $1 \leq k \leq mN - 1$. Because $\sin(\theta) = \sin(\pi - \theta)$, every non-zero eigenvalue corresponding to $\theta_k(m, N) \neq \frac{\pi}{2}$ is double. Because all eigenvalues $\lambda \in i\mathbb{R}_+$ have a definite Krein signature by Lemma 3 and the sign of $\sigma_n^{(1)}$ in (3.31) is the same for both eigenvalues with $\sin(\theta) =$

$\sin(\pi - \theta)$, the double eigenvalues $\lambda \in i\mathbb{R}$ are structurally stable with respect to parameter continuations [4] in the sense that they split along the imaginary axis beyond the leading-order perturbation theory.

Remark 9. *The argument based on the Krein signature does not cover the case of double real eigenvalues $\Lambda \in \mathbb{R}_+$, which may split off the real axis to the complex domain. However, both real and complex eigenvalues contribute to the count of unstable eigenvalues with the account of their multiplicities.*

It remains to address the issue that the first-order perturbation theory uses computations of V''', which is not a continuous function of its argument. To deal with this issue, we use a renormalization technique. We note that if (u_*, w_*) is a solution of the differential advance-delay equations (1.14) given by Theorem 1, then

$$\begin{aligned} \dddot{u}_*(\tau) &= V''(\varepsilon w_*(\tau) - u_*(\tau))(\varepsilon \dot{w}_*(\tau) - \dot{u}_*(\tau)) \\ &\quad -V''(u_*(\tau) - \varepsilon w_*(\tau - 2q))(\dot{u}_*(\tau) - \varepsilon \dot{w}_*(\tau - 2q)), \end{aligned} \tag{3.33}$$

where the right-hand side is a continuous function of τ.

Using (3.33), we substitute

$$U_{2n-1} = c_{2n-1}\dot{u}_*(\tau + 2qn) + \mathcal{U}_{2n-1}, \quad W_{2n} = \mathcal{W}_{2n},$$

for an arbitrary choice of $\{c_{2n-1}\}_{n\in\mathbb{Z}}$, into the linear eigenvalue problem (3.7)

and obtain:

$$\begin{cases} \ddot{\mathcal{U}}_{2n-1} + 2\lambda\dot{\mathcal{U}}_{2n-1} + \lambda^2\mathcal{U}_{2n-1} = V''(\varepsilon w_*(\tau+2qn) - u_*(\tau+2qn))(\varepsilon\mathcal{W}_{2n} - \mathcal{U}_{2n-1}) \\ \qquad\qquad - V''(u_*(\tau+2qn) - \varepsilon w_*(\tau+2qn-2q))(\mathcal{U}_{2n-1} - \varepsilon\mathcal{W}_{2n-2}), \\ \qquad\qquad - (2\lambda\ddot{u}_*(\tau+2qn) + \lambda^2\dot{u}_*(\tau+2qn))c_{2n-1} \\ \qquad\qquad - \varepsilon V''(\varepsilon w_*(\tau+2qn) - u_*(\tau+2qn))\dot{w}_*(\tau+2qn)c_{2n-1} \\ \qquad\qquad - \varepsilon V''(u_*(\tau+2qn) - \varepsilon w_*(\tau+2qn-2q))\dot{w}_*(\tau+2qn-2q)c_{2n-1}, \\ \ddot{\mathcal{W}}_{2n} + 2\lambda\dot{\mathcal{W}}_{2n} + \lambda^2\mathcal{W}_{2n} = \varepsilon V''(u_*(\tau+2qn+2q) - \varepsilon w_*(\tau+2qn))(\mathcal{U}_{2n+1} - \varepsilon\mathcal{W}_{2n}) \\ \qquad\qquad - \varepsilon V''(\varepsilon w_*(\tau+2qn) - u_*(\tau+2qn))(\varepsilon\mathcal{W}_{2n} - \mathcal{U}_{2n-1}) \\ \qquad\qquad + \varepsilon V''(u_*(\tau+2qn+2q) - \varepsilon w_*(\tau+2qn))\dot{u}_*(\tau+2qn+2q)c_{2n-1} \\ \qquad\qquad + \varepsilon V''(\varepsilon w_*(\tau+2qn) - u_*(\tau+2qn))\dot{u}_*(\tau+2qn)c_{2n-1}. \end{cases} \tag{3.34}$$

When we repeat decompositions of the first-order perturbation theory, we write

$$\begin{aligned} \lambda &= \varepsilon\lambda^{(1)} + \varepsilon^2\lambda^{(2)} + \mathrm{o}(\varepsilon^2), \\ \mathcal{U}_{2n-1} &= \varepsilon\mathcal{U}_{2n-1}^{(1)} + \varepsilon^2\mathcal{U}_{2n-1}^{(2)} + \mathrm{o}(\varepsilon^2), \\ \mathcal{W}_{2n} &= a_{2n} + \varepsilon\mathcal{W}_{2n}^{(1)} + \varepsilon^2\mathcal{W}_{2n}^{(2)} + \mathrm{o}(\varepsilon^2), \end{aligned}$$

for an arbitrary choice of $\{a_{2n}\}_{n\in\mathbb{Z}}$. Substituting this decomposition to system (3.34), we obtain equations at the $\mathcal{O}(\varepsilon)$ and $\mathcal{O}(\varepsilon^2)$ orders, which do not require computations of V'''. Hence, the system of difference equations (3.19) is justified and the splitting of the eigenvalues λ at the first order of the perturbation theory obeys roots of the characteristic equation (3.28). Persistence of roots beyond the $\mathrm{o}(\varepsilon^2)$ order holds by the standard perturbation theory for isolated eigenvalues of the Floquet matrix. The proof of Theorem 2 is complete.

Chapter 4

Numerical Results

In order to perform numerical analysis of the 2π-periodic travelling waves (1.12) in the case $q = \frac{\pi}{N}$ where $N \in \mathbb{Z}_+$, we rewrite the system of $2N$ differential equations (1.4) in the form:

$$\begin{cases} \ddot{u}_{2n-1}(t) = (\varepsilon w_{2n}(t) - u_{2n-1}(t))_+^\alpha - (u_{2n-1}(t) - \varepsilon w_{2n-2}(t))_+^\alpha, \\ \ddot{w}_{2n}(t) = \varepsilon(u_{2n-1}(t) - \varepsilon w_{2n}(t))_+^\alpha - \varepsilon(\varepsilon w_{2n}(t) - u_{2n+1}(t))_+^\alpha, \end{cases} \quad 1 \le n \le N, \tag{4.1}$$

subject to periodic boundary conditions

$$u_{-1} = u_{2N-1}, \quad u_{2N+1} = u_1, \quad w_0 = w_{2N}, \quad w_{2N+2} = w_2. \tag{4.2}$$

The linearized system is given by

$$\begin{cases} \ddot{\tilde{u}}_{2n-1}(t) = (\varepsilon w_{2n}(t) - u_{2n-1}(t))_+^\alpha(\varepsilon\tilde{w}_{2n}(t) - \tilde{u}_{2n-1}(t)) \\ \qquad\qquad - (u_{2n-1}(t) - \varepsilon w_{2n-2}(t))_+^{\alpha-1}(\tilde{u}_{2n-1}(t) - \varepsilon\tilde{w}_{2n-2}(t)), \\ \ddot{\tilde{w}}_{2n}(t) = \varepsilon(u_{2n-1}(t) - \varepsilon w_{2n}(t))_+^\alpha(\tilde{u}_{2n-1}(t) - \varepsilon\tilde{w}_{2n}(t)) \\ \qquad\qquad - \varepsilon(\varepsilon w_{2n}(t) - u_{2n+1}(t))_+^\alpha(\varepsilon\tilde{w}_{2n}(t) - \tilde{u}_{2n+1}(t)), \end{cases} \quad 1 \le n \le N, \tag{4.3}$$

The 2π-periodic travelling waves (1.12) correspond to 2π-periodic solutions of system (4.1) satisfying the reduction

$$\begin{aligned} u_{2n+1}(t) &= u_{2n-1}\left(t+\tfrac{2\pi}{N}\right), \\ w_{2n+2}(t) &= w_{2n}\left(t+\tfrac{2\pi}{N}\right), \end{aligned} \qquad t\in\mathbb{R}, \quad 1\le n\le N. \tag{4.4}$$

For uniqueness, we require u_1 be an odd function, $u_1(t) = -u_1(-t)$ such that

$$u_1(0) = 0 \quad \text{and} \quad \dot{u}_1(0) > 0.$$

By Theorem 1 for every $N \in \mathbb{Z}_+$, the travelling wave solution satisfying (4.4) exists and is unique at least for small values of ε. We can continue the limiting solutions from $\varepsilon = 0$ with respect to parameter ε numerically along this branch all the way to the limit of equal mass ratio, $\varepsilon = 1$.

4.1 Existence of Periodic Travelling Waves

In order to numerically compute the 2π-periodic travelling wave solutions to the nonlinear system (4.1) we use the classical shooting method [12]. Our shooting parameters are given by the set of initial conditions

$$\{u_{2n-1}(0), \dot{u}_{2n-1}(0), w_{2n}(0), \dot{w}_{2n}(0)\}_{1\le n\le N}.$$

Since $u_1(0) = 0$, we have a set of $2N-1$ shooting parameters. However, for a fixed N, we can use the symmetries of the nonlinear ODE system (4.1) to reduce the number of shooting parameters needed for approximation of solutions satisfying the travelling wave reductions (4.4).

For clarity, we give the examples of four particles ($N = 2$ or $q = \frac{\pi}{2}$),

six particles ($N = 3$ or $q = \frac{\pi}{3}$) and eight particles ($N = 4$ or $q = \frac{\pi}{4}$) explicitly. For $N = 2$, we can write the nonlinear ODE system (4.1) as

$$\begin{cases} \ddot{u}_1(t) = (\varepsilon w_4(t) - u_1(t))_+^\alpha - (u_1(t) - \varepsilon w_2(t))_+^\alpha, \\ \ddot{w}_2(t) = \varepsilon[(u_1(t) - \varepsilon w_2(t))_+^\alpha - (\varepsilon w_2(t) - u_3(t))_+^\alpha], \\ \ddot{u}_3(t) = (\varepsilon w_2(t) - u_3(t))_+^\alpha - (u_3(t) - \varepsilon w_4(t))_+^\alpha, \\ \ddot{w}_4(t) = \varepsilon[(u_3(t) - \varepsilon w_4(t))_+^\alpha - (\varepsilon w_4(t) - u_1(t))_+^\alpha]. \end{cases} \tag{4.5}$$

We seek 2π-periodic functions satisfying the travelling wave reduction

$$u_3(t) = u_1(t + \pi), \quad w_4(t) = w_2(t + \pi). \tag{4.6}$$

The system (4.5) is invariant with respect to the transformation

$$u_1(t) = -u_1(-t), \quad w_2(t) = -w_4(-t), \quad u_3(t) = -u_3(-t). \tag{4.7}$$

A 2π-periodic solution of system (4.5) satisfying (4.7) must also satisfy $u_1(\pi) = u_3(\pi) = 0$ and $w_2(\pi) = -w_4(\pi)$. In addition, a solution satisfying (4.6) must also satisfy $w_4(\pi) = w_2(0)$.

An approximation of a solution to the system (4.5) satisfying (4.7) needs only four shooting parameters, (a_1, a_2, a_3, a_4), in the initial condition,

$$\begin{aligned} u_1(0) = 0, \quad \dot{u}_1(0) = a_1, \quad w_2(0) = a_2, \quad \dot{w}_2(0) = a_3, \\ u_3(0) = 0, \quad \dot{u}_3(0) = a_4, \quad w_4(0) = -a_2, \quad \dot{w}_4(0) = a_3. \end{aligned}$$

The solution of the initial-value problem corresponds to a 2π-periodic travel-

ling wave solution only if the following four conditions are satisfied:

$$u_1(\pi) = 0, \quad w_2(\pi) + w_4(\pi) = 0, \quad w_2(0) - w_4(\pi) = 0, \quad u_3(\pi) = 0.$$

These four conditions fully specify the shooting method for the four parameters (a_1, a_2, a_3, a_4). Additionally, the reductions (4.6) and (4.7) also require the conditions

$$\dot{w}_2(\pi) - \dot{w}_4(\pi) = 0, \quad \dot{w}_2(0) - \dot{w}_4(\pi) = 0,$$

but these conditions are redundant for the shooting method. We have been checking these conditions a posteriori, when the shooting method has converged to a solution.

The error of the shooting method is generated from the error of the ODE solver and the error in finding zeros of the above functions. We use the built-in MATLAB function `ode113` on the interval $[0, \pi]$ as the ODE solver and then use the transformation (4.7) to extend the solution on the interval $[-\pi, 0]$ and hence to continue to a full period $[0, 2\pi]$.

Figure 2 shows the three solution branches obtained by the shooting method. The first solution branch (labeled Branch 1) exists for all $\varepsilon \in [0, 1]$ and is shown in the top right panel for $\varepsilon = 1$. This branch coincides with the exact solution (1.24) found analytically. The error in the supremum norm between the numerical and exact solutions $\|u_1 - \varphi\|_{L^\infty}$ can be found in Table 5.1.

`AbsTol` of Shooting Method	`AbsTol` of ODE solver	L^∞ error
$\mathcal{O}(10^{-12})$	$\mathcal{O}(10^{-15})$	4.5×10^{-14}
	$\mathcal{O}(10^{-10})$	3.0×10^{-11}
$\mathcal{O}(10^{-8})$	$\mathcal{O}(10^{-15})$	4.5×10^{-14}
	$\mathcal{O}(10^{-10})$	3.0×10^{-11}

Table 5.1: Error between numerical and exact solutions for branch 1.

The top left panel of Figure 4.1 shows $w_2(0)$ versus ε. A pitchfork bifurcation occurs at $\varepsilon = \varepsilon_0 \approx 0.72$ and results in two symmetrically reflected branches (labeled Branch 2 and Branch 2'). These branches with $w_2(0) \neq 0$ extend to $\varepsilon = 1$ (bottom panels) where the two travelling wave solutions of the monomer chain (1.6) are recovered. The solution of Branch 2 satisfies the travelling wave reduction $U_{n+1}(t) = U_n(t+q)$ and was previously obtained numerically by James [15]. The solution of Branch 2' satisfies the travelling wave reduction $U_{n+1}(t) = U_n(t-q)$ and was approximated numerically by Starosvetsky and Vakakis [26].

For $N = 2$ ($q = \frac{\pi}{2}$) the solution of Branch 2' given by $\{\tilde{u}_{2n-1}, \tilde{w}_{2n}\}_{n\in\{1,2\}}$ can be obtained from the solution of Branch 2 given by $\{u_{2n-1}, w_{2n}\}_{n\in\{1,2\}}$ through the symmetry

$$\tilde{u}_1(t) = -u_3(t), \quad \tilde{w}_2(t) = -w_2(t)$$
$$\tilde{u}_3(t) = -u_1(t), \quad \tilde{w}_4(t) = -w_2(t).$$

This symmetry holds for all $\varepsilon > 0$ although it is clear that both solutions 2 and 2' only exist for $\varepsilon \in (\varepsilon_0, 1]$ due to the pitchfork bifurcation at $\varepsilon = \varepsilon_0 \approx 0.72$. The solution of Branch 1 is the invariant symmetry reduction $\tilde{u}_{2n-1} = u_{2n-1}$, $\tilde{w}_{2n} = w_{2n}$, so that $w_2(t) = w_4(t) = 0$ is satisfied for all t.

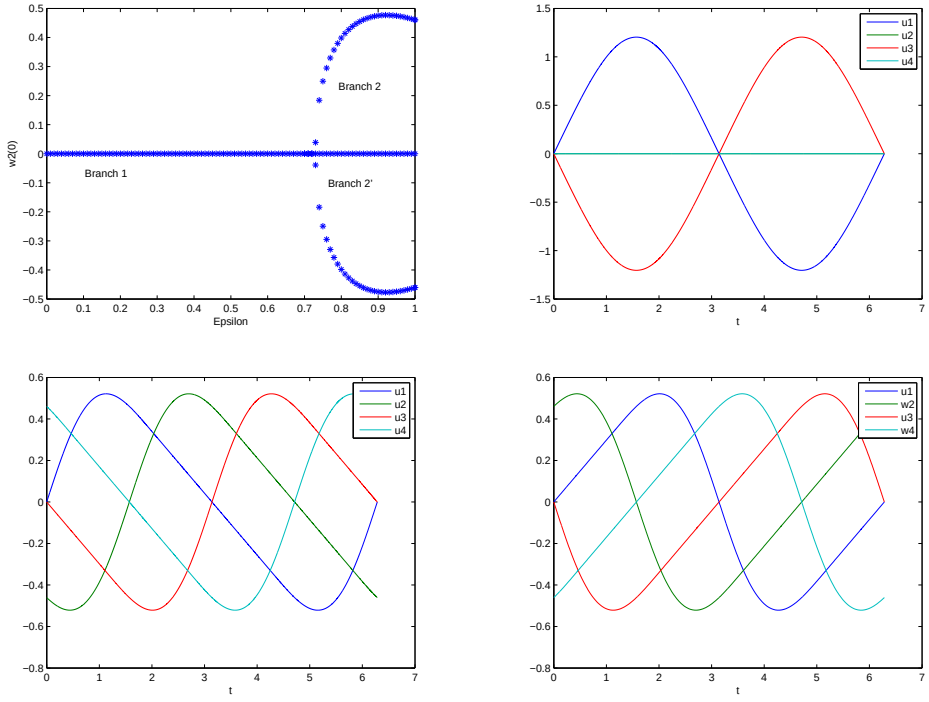

Figure 4.1: Travelling wave solutions for $N = 2$: the solution of the dimer chain continued from $\varepsilon = 0$ to $\varepsilon = 1$ (top right) and two solutions of the monomer chain at $\varepsilon = 1$ (bottom left and right). The top left panel shows the value of $w_2(0)$ for all three solutions branches versus ε.

In the case of six particles ($N = 3$ or $q = \frac{\pi}{3}$), the nonlinear ODE system (4.1) can be explicitly written as

$$\begin{cases} \ddot{u}_1(t) = (\varepsilon w_6(t) - u_1(t))_+^\alpha - (u_1(t) - \varepsilon w_2(t))_+^\alpha, \\ \ddot{w}_2(t) = \varepsilon[(u_1(t) - \varepsilon w_2(t))_+^\alpha - (\varepsilon w_2(t) - u_3(t))_+^\alpha], \\ \ddot{u}_3(t) = (\varepsilon w_2(t) - u_3(t))_+^\alpha - (u_3(t) - \varepsilon w_4(t))_+^\alpha, \\ \ddot{w}_4(t) = \varepsilon[(u_3(t) - \varepsilon w_4(t))_+^\alpha - (\varepsilon w_4(t) - u_5(t))_+^\alpha], \\ \ddot{u}_5(t) = (\varepsilon w_4(t) - u_5(t))_+^\alpha - (u_5(t) - \varepsilon w_6(t))_+^\alpha, \\ \ddot{w}_6(t) = \varepsilon[(u_5(t) - \varepsilon w_6(t))_+^\alpha - (\varepsilon w_6(t) - u_1(t))_+^\alpha]. \end{cases} \tag{4.8}$$

We are looking for 2π-periodic functions satisfying the travelling wave reduc-

tion:

$$\begin{aligned} u_5(t) &= u_3\left(t+\tfrac{2\pi}{3}\right) = u_1\left(t+\tfrac{4\pi}{3}\right), \\ w_6(t) &= w_4\left(t+\tfrac{2\pi}{3}\right) = w_2\left(t+\tfrac{4\pi}{3}\right). \end{aligned} \tag{4.9}$$

It can be seen that system (4.8) is invariant under the following transformation:

$$\begin{aligned} u_1(-t) &= -u_1(t), \quad w_2(-t) = -w_6(t), \\ u_3(-t) &= -u_5(t), \quad w_4(-t) = -w_4(t). \end{aligned} \tag{4.10}$$

A 2π-periodic solution to system (4.8) satisfying (4.10) must also satisfy the conditions $u_1(\pi) = w_4(\pi) = 0$, $w_2(\pi) = -w_6(\pi)$, and $u_3(\pi) = -u_5(\pi)$. The constraints of the travelling wave reduction (4.9) force the conditions: $u_3(\pi) = -u_1\left(\frac{\pi}{3}\right)$ and $w_4(\pi) = -w_2\left(\frac{\pi}{3}\right)$.

To approximate a solution of the initial-value problem for the system (4.8) satisfying (4.10) numerically, we only need six shooting parameters, $(a_1, a_2, a_3, a_4, a_5, a_6)$, in the initial condition:

$$\begin{gathered} u_1(0) = 0, \quad \dot{u}_1(0) = a_1, \quad w_2(0) = a_2, \quad \dot{w}_2(0) = a_3, \\ u_3(0) = a_4, \quad \dot{u}_3(0) = a_5, \quad w_4(0) = 0, \quad \dot{w}_4(0) = a_6, \\ u_5(0) = -a_4, \quad \dot{u}_5(0) = a_5, \quad w_6(0) = -a_2, \quad \dot{w}_6(0) = a_3. \end{gathered}$$

This solution corresponds to a 2π-periodic travelling wave solution only if it satisfies the following six conditions:

$$\begin{gathered} u_1(\pi) = 0, \quad w_2(\pi) + w_6(\pi) = 0, \quad u_3(\pi) + u_5(\pi) = 0, \\ u_1\left(\tfrac{\pi}{3}\right) + u_3(\pi) = 0 \quad w_2\left(\tfrac{\pi}{3}\right) + w_4(\pi) = 0, \quad w_4(\pi) = 0. \end{gathered}$$

Reductions (4.9) and (4.10) also require we satisfy the conditions

$$\dot{u}_3(\pi) - \dot{u}_5(\pi) = 0, \quad \dot{u}_1\left(\frac{\pi}{3}\right) - \dot{u}_3(\pi) = 0,$$
$$\dot{w}_2(\pi) - \dot{w}_6(\pi) = 0 \quad \dot{w}_2\left(\frac{\pi}{3}\right) - \dot{w}_4(\pi) = 0.$$

These conditions are redundant for the shooting method and are checked a posteriori after the shooting method has converged on a solution.

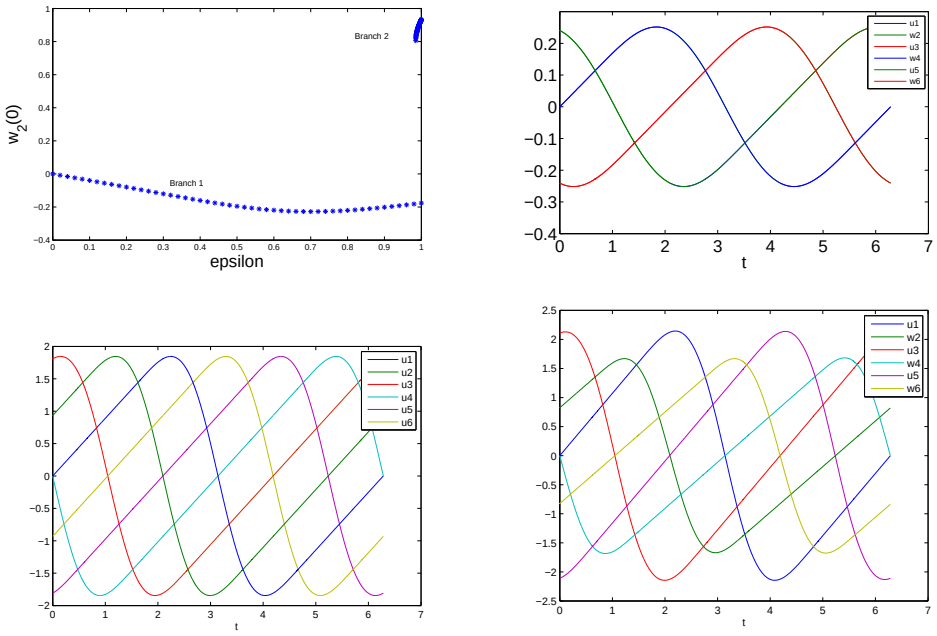

Figure 4.2: Travelling wave solutions for $N = 3$: the solution of branch 1 is continued from $\varepsilon = 0$ to $\varepsilon = 1$ (top right) and the solution of branch 2 is continued from $\varepsilon = 1$ (bottom left) to $\varepsilon = 0.985$ (bottom right). The top left panel shows the value of $w_2(0)$ for solution branches 1 and 2 versus ε.

Figure 4.2 shows two solution branches obtained by the shooting method for $N = 3$. Again, $w_2(0)$ is plotted versus ε. Branch 1 is continued from $\varepsilon = 0$ to $\varepsilon = 1$ (top right) without any pitchfork bifurcation in $\varepsilon \in (0, 1)$. Branch 2 is continued from $\varepsilon = 1$ (bottom left) starting with a numerical solution

of the monomer chain (1.6) satisfying the reduction $U_{n+1}(t) = U_n\left(t+\frac{\pi}{3}\right)$ to $\varepsilon = 0.985$ (bottom right), where the branch terminates according to our shooting method. We have not been able so far to detect numerically any other branch of travelling wave solutions near branch 2 for $\varepsilon = 0.985$, hence the nature of this bifurcation will remain open for further studies.

For the case of eight particles ($N = 4$ or $q = \frac{\pi}{4}$), the nonlinear ODE system (4.1) can be written explicitly as

$$\begin{cases} \ddot{u}_1(t) = (\varepsilon w_8(t) - u_1(t))_+^\alpha - (u_1(t) - \varepsilon w_2(t))_+^\alpha, \\ \ddot{w}_2(t) = \varepsilon[(u_1(t) - \varepsilon w_2(t))_+^\alpha - (\varepsilon w_2(t) - u_3(t))_+^\alpha], \\ \ddot{u}_3(t) = (\varepsilon w_2(t) - u_3(t))_+^\alpha - (u_3(t) - \varepsilon w_4(t))_+^\alpha, \\ \ddot{w}_4(t) = \varepsilon[(u_3(t) - \varepsilon w_4(t))_+^\alpha - (\varepsilon w_4(t) - u_5(t))_+^\alpha], \\ \ddot{u}_5(t) = (\varepsilon w_4(t) - u_5(t))_+^\alpha - (u_5(t) - \varepsilon w_6(t))_+^\alpha, \\ \ddot{w}_6(t) = \varepsilon[(u_5(t) - \varepsilon w_6(t))_+^\alpha - (\varepsilon w_6(t) - u_7(t))_+^\alpha], \\ \ddot{u}_7(t) = (\varepsilon w_6(t) - u_7(t))_+^\alpha - (u_7(t) - \varepsilon w_8(t))_+^\alpha, \\ \ddot{w}_8(t) = \varepsilon[(u_7(t) - \varepsilon w_8(t))_+^\alpha - (\varepsilon w_8(t) - u_1(t))_+^\alpha]. \end{cases} \tag{4.11}$$

We seek 2π-periodic functions which satisfy the travelling wave reduction:

$$\begin{aligned} u_7(t) &= u_5\left(t+\tfrac{\pi}{2}\right) = u_3\left(t+\pi\right) = u_1\left(t+\tfrac{3\pi}{2}\right), \\ w_8(t) &= w_6\left(t+\tfrac{\pi}{2}\right) = w_4\left(t+\pi\right) = w_2\left(t+\tfrac{3\pi}{2}\right). \end{aligned} \tag{4.12}$$

Moreover, system (4.11) is invariant with respect to the transformation:

$$\begin{aligned} &u_1(-t) = -u_1(t), \quad u_3(-t) = -u_7(t), \quad u_5(-t) = -u_5(t) \\ &w_2(-t) = -w_8(t), \quad w_4(-t) = -w_6(t). \end{aligned} \tag{4.13}$$

A 2π-periodic solution to system (4.11) satisfying (4.13) must satisfy the conditions $u_1(\pi) = u_5(\pi) = 0$, $w_2(\pi) = -w_8(\pi)$, $u_3(\pi) = -u_7(\pi)$, and

$w_4(\pi) = -w_6(\pi)$. The travelling wave reduction (4.12) yield the conditions $w_2(0) = w_6(\pi)$, $u_3(0) = u_7(\pi)$, and $w_8(0) = w_4(\pi)$.

To approximate a solution to the initial value problem for the nonlinear system (4.11) satisfying (4.12) and (4.13) we need eight shooting parameters $(a_1, a_2, a_3, a_4, a_5, a_6, a_7, a_8)$ in the initial condition:

$$\begin{gathered} u_1(0) = 0, \quad \dot{u}_1(0) = a_1, \quad w_2(0) = a_2, \quad \dot{w}_2(0) = a_3, \\ u_3(0) = a_4, \quad \dot{u}_3(0) = a_5, \quad w_4(0) = a_6, \quad \dot{w}_4(0) = a_7, \\ u_5(0) = 0, \quad \dot{u}_5(0) = a_8, \quad w_6(0) = -a_6, \quad \dot{w}_6(0) = a_7, \\ u_7(0) = -a_4, \quad \dot{u}_7(0) = a_5, \quad w_8(0) = -a_2, \quad \dot{w}_8(0) = a_3. \end{gathered}$$

This solution corresponds to a 2π-periodic travelling wave solution only if it satisfies the following eight conditions:

$$\begin{gathered} u_1(\pi) = 0, \quad w_2(\pi) + w_8(\pi) = 0, \quad u_3(\pi) + u_7(\pi) = 0, \quad w_4(\pi) + w_6(\pi) = 0, \\ w_2(0) - w_6(\pi) = 0, \quad u_3(0) - u_7(\pi) = 0, \quad w_8(0) - w_4(\pi) = 0, \quad u_5(\pi) = 0. \end{gathered}$$

These eight conditions determine the shooting method for the eight parameters $(a_1, a_2, a_3, a_4, a_5, a_6, a_7, a_8)$. Again, there are additional conditions, namely,

$$\begin{gathered} \dot{w}_2(\pi) + \dot{w}_8(\pi) = 0, \quad \dot{u}_3(\pi) + \dot{u}_7(\pi) = 0, \quad \dot{w}_4(\pi) + \dot{w}_6(\pi) = 0, \\ \dot{w}_2(0) - \dot{w}_6(\pi) = 0, \quad \dot{u}_3(0) - \dot{u}_7(\pi) = 0, \quad \dot{w}_8(0) - \dot{w}_4(\pi) = 0. \end{gathered}$$

These conditions are redundant for the shooting method and are checked aposteriori.

Figure 4.3 shows the bifurcation plot for $N = 4$. It is similar to that

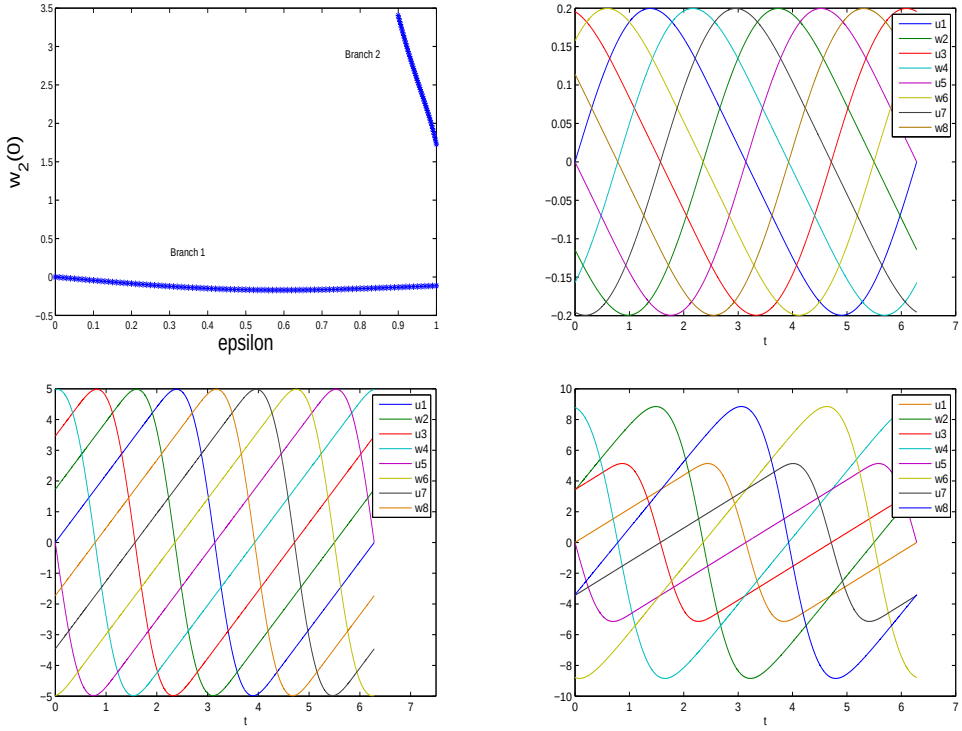

Figure 4.3: Travelling wave solutions for $N = 4$: the solution of branch 1 continued from $\varepsilon = 0$ to $\varepsilon = 1$ (top right) and the solution of branch 1 continued from $\varepsilon = 1$ (bottom left) to $\varepsilon = 0.9$ (bottom right). The top left panel shows the value of $w_2(0)$ for solution branches 1 and 2 versus ε.

of $N = 3$ in that there is no pitchfork bifurcation, and only two branches are shown: Branch 1 is continued from the anticontinuum limit, $\varepsilon = 0$, and Branch 2 is continued from the limit of equal masses, $\varepsilon = 1$. We note that this bifurcation diagram is topologically different from that of $N = 3$ in that $w_2(0)$ for Branch 2 increases for smaller values of ε whereas for $N = 3$, $w_2(0)$ decreases for smaller values of ε. Branch 2 terminates at $\varepsilon = \varepsilon_0 \approx 0.9$. At $\varepsilon = 1$ the solution satisfies the reduction $U_{n+1}(t) = U_n\left(t + \frac{\pi}{4}\right)$ and is a solution to the monomer chain (1.6).

4.2 Stability of Periodic Travelling Waves

To determine stability of periodic travelling wave solutions of the granular dimer chain (1.4), we compute Floquet multipliers of the monodromy matrix for the linearized system (3.1). To do this, we use the travelling wave solution obtained with the shooting method and the MATLAB function `ode113` to compute the fundamental matrix solution of the linearized system (3.1) on the interval $[0, 2\pi]$.

By Theorem 2, the travelling waves of Branch 1 for $N = 2$ $\left(q = \frac{\pi}{2}\right)$ are unstable for small values of ε. Figure 4.4 (top) shows the real and imaginary parts of the characteristic exponents associated with Branch 1 for all values of $\varepsilon \in [0, 1]$. We show only positive values of the characteristic exponents since the negative values are symmetric. Moreover, $\mathrm{Im}(\lambda)$ is shown in the interval $\left[0, \frac{1}{2}\right)$ because of the 1-periodicity of characteristic exponents along the imaginary axis.

Taking advantage of periodic boundary conditions we can close the system of linearized equations (3.1) for $N = 2$ at four second-order differential equations. For Branch 1, the equations produce eight characteristic exponents: exponent $\lambda = 0$ of multiplicity 4 for small $\varepsilon > 0$, one pair of real λ which persist for all $\varepsilon \in [0, 1]$. The final pair of λ is purely imaginary for $\varepsilon \in [0, \varepsilon_0)$ at which point the pair coalesces and splits along the real axis, creating a second pair of real λ for $\varepsilon \in (\varepsilon_0, 1]$. We can conclude that Branch 1 for $N = 2$ is unstable for all $\varepsilon \in [0, 1]$. The nonzero pairs of λ bifurcate from the anti-continuum limit, $\varepsilon = 0$, according to the roots of the characteristic polynomial (3.28) for $\theta = \frac{\pi}{2}$. The asymptotic approximations are shown in the top panels of Figure 4.4 by solid lines. We note the excellent agreement between the asymptotic approximation and numerical data.

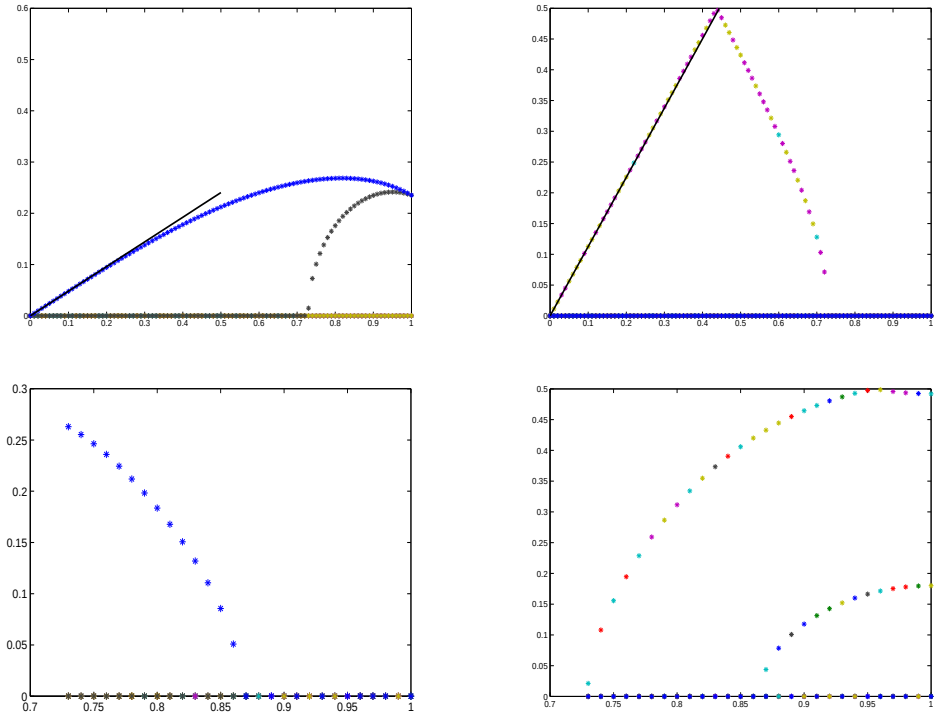

Figure 4.4: Real (left) and imaginary (right) parts of the characteristic exponents λ versus ε for $N = 2$ for branch 1 (top) and branch 2 (bottom).

The bottom panels of Figure 4.4 show real and imaginary parts of characteristic exponents λ associated with Branch 2 (and Branch 2' by symmetry) for all values of $\varepsilon \in [\varepsilon_0, 1]$. We see that these periodic travelling waves are spectrally stable near $\varepsilon = 1$, in agreement with numerical results presented by James [15]. As ε is decreased, we lose spectral stability near $\varepsilon = \varepsilon_1 \approx 0.86$. This occurs because of a coalescence of a pair of purely imaginary characteristic exponents λ which creates a pair of real characteristic exponents λ for $\varepsilon < \varepsilon_1$. The two solution branches (Branch 2 and 2') annihilate each other as a result of the pitchfork bifurcation at $\varepsilon = \varepsilon_0 \approx 0.72$ which is also induced by the coalescence of the second pair of purely imaginary characteristic exponents

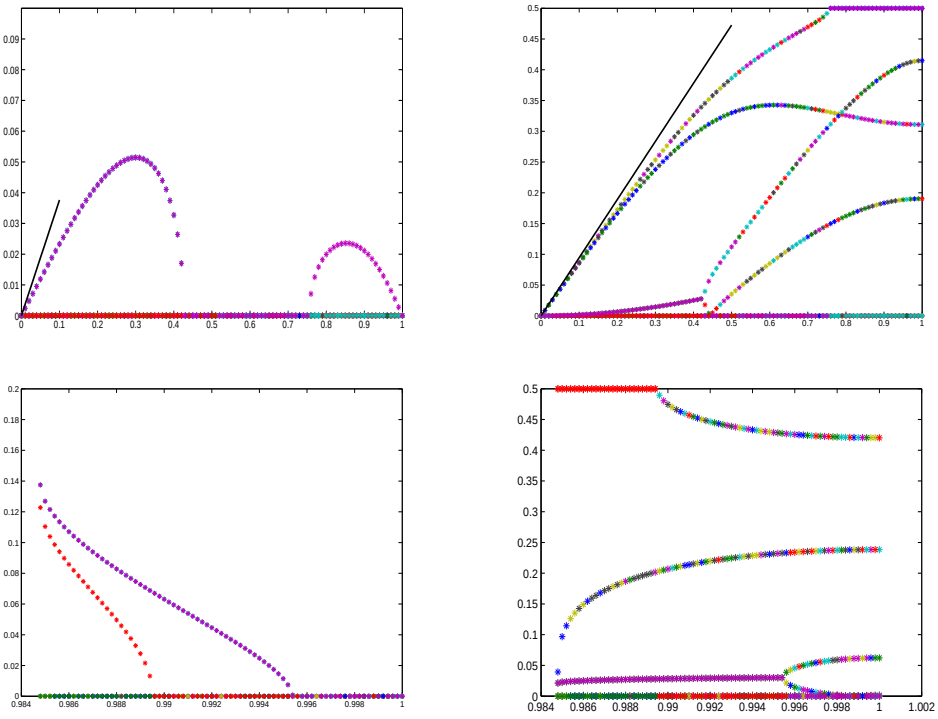

Figure 4.5: Real (left) and imaginary (right) parts of the characteristic exponents λ versus ε for $N = 3$ for branch 1 (top) and branch 2 (bottom).

λ.

For $N = 3$, we are able to close the system of linearized equations (3.1) at six second-order linearized equations because of periodic boundary conditions. Barring the characteristic exponent $\lambda = 0$ of multiplicity four, we have eight nonzero characteristic exponents λ. The characteristic polynomial (3.28) with $\theta = \frac{\pi}{3}$ and $\theta = \frac{2\pi}{3}$ predicts a double pair of real λ and a double pair of purely imaginary λ. The top panel of Figure 4.5 shows Re(λ) (left) and Im(λ) (left) for solutions of Branch 1. The double pair of purely imaginary λ split along the imaginary axis for small $\varepsilon > 0$. In contrast, the double pair of real λ split along the transverse direction and create a quartet of complex-

valued λ for small $\varepsilon > 0$. These complex λ approach the imaginary axis at $\varepsilon = \varepsilon_1 \approx 0.43$ in a Neimark-Sacker bifurcation and then split safely along the imaginary axis as two pairs of purely imaginary λ for $\varepsilon > \varepsilon_1$. We also have one pair of purely imaginary λ continued from $\varepsilon = 0$ approaching the line $\pm\frac{i}{2}$ at $\varepsilon = \varepsilon_2 \approx 0.72$. The line $\pm\frac{i}{2}$ corresponds to a Floquet multiplier at -1, that is, a period-doubling bifurcation takes place at $\varepsilon = \varepsilon_2$. The pair of imaginary λ splits in a complex plane for $\varepsilon > \varepsilon_2$ (the corresponding Floquet multipliers are real and negative). In summary, we have that the periodic travelling wave of Branch 1 for $N = 3$ has an island of stability for $\varepsilon \in (\varepsilon_1, \varepsilon_2)$ but is unstable near $\varepsilon = 0$ and $\varepsilon = 1$.

The bottom of Figure 4.5 shows $\mathrm{Re}(\lambda)$ (left) and $\mathrm{Im}(\lambda)$ (right) for solutions of Branch 2. Such a solution only exists for $\varepsilon \in [\varepsilon_*, 1]$, where $\varepsilon_* \approx 0.985$. Near $\varepsilon = 1$, we see that all four pairs of characteristic exponents, λ, are purely imaginary. This corresponds to numerical stability of travelling waves in monomer chains [15]. Two pairs coalesce at $\varepsilon \approx 0.995$ and split in a complex quartet of characteristic exponents (resulting in a Neimark-Sacker bifurcation). Another purely imaginary pair of λ approach the line $\pm\frac{i}{2}$ at $\varepsilon \approx 0.989$. The pair then splits in a complex quartet (resulting in a period doubling bifurcation). The final remaining pair of purely imaginary λ crosses zero near $\varepsilon = \varepsilon_* \approx 0.985$. This picture suggests that the termination of Branch 2 is related to a local bifurcation. Using the current methods, we are not able to numerically identify any other branch of travelling wave solutions in the neighbourhood of Branch 2 for $\varepsilon \approx \varepsilon_*$.

We recall that the coefficient M_1 changes sign at $q \approx 0.915$, as seen in Figure 3.1. Considering this, the characteristic polynomial (3.28) for any value of θ predicts pairs of purely imaginary λ for $N \geq 4$. For $N = 4$, it predicts two double pairs for $\theta = \frac{\pi}{4}$ and $\theta = \frac{3\pi}{4}$ and two single pairs for $\theta = \frac{\pi}{2}$.

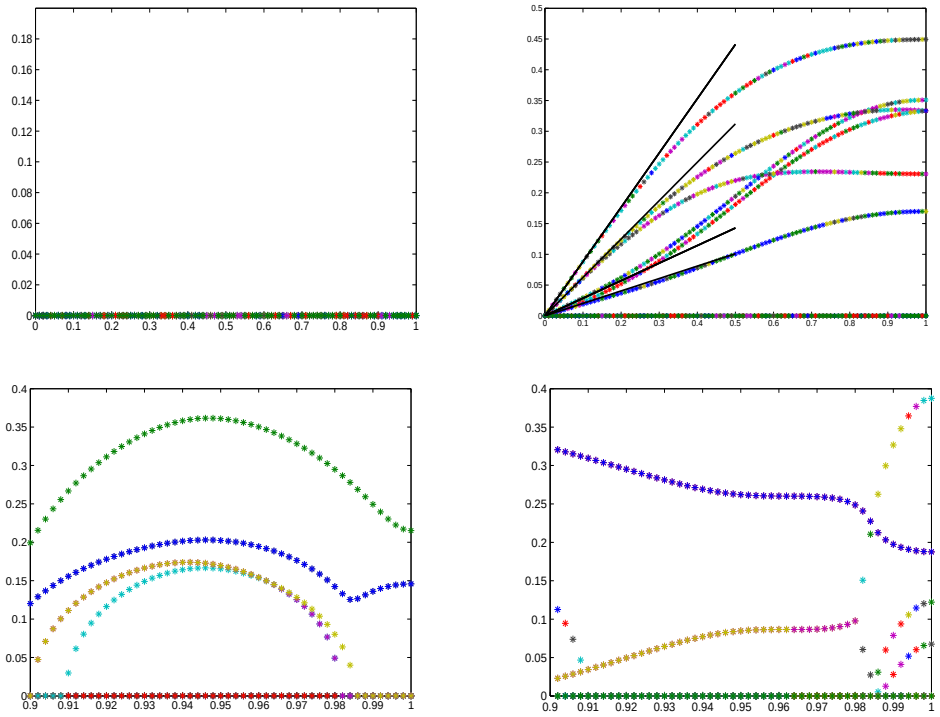

Figure 4.6: Real (left) and imaginary (right) parts of the characteristic exponents λ versus ε for $N = 4$ for branch 1 (top) and branch 2 (bottom).

This prediction is realized in the top panel of Figure 4.6 for $N = 4$ or $q = \frac{\pi}{4}$. Again, neglecting the characteristic exponent $\lambda = 0$ of multiplicity four, we have twelve nonzero λ. We see from Figure 4.6 that the result of Theorem 2 holds as all double pairs of λ split along the imaginary axis for small $\varepsilon > 0$. The periodic travelling waves for $N = 4$ remain stable for all $\varepsilon \in [0, 1]$. The figure also illustrates the validity of the asymptotic approximations (solid lines) obtained from the roots of the characteristic polynomial (3.28).

It is indeed interesting that Figure 4.6 shows safe coalescence of characteristic exponents for larger values of ε. We recall from Remark 8 that the characteristic exponents have opposite Krein signature for small values of ε

such that larger exponents on Figure 4.6 have negative Krein signature σ and smaller exponents have positive Krein signature σ. It is typical to observe instabilities arise after the coalescence of two purely imaginary eigenvalues of opposite Krein signature [20], but this happens when the double eigenvalue at the coalescence point is not semi-simple. When the double eigenvalues are semi-simple, instabilities do not arise [3]. This is what we observe in Figure 4.6. After coalescence, for larger values of ε, the purely imaginary characteristic exponents λ reappear as simple exponents with opposite Krein signature; i.e. the exponents with positive Krein signature are now above those exponents with negative Krein signature.

The bottom panel of Figure 4.6 shows $\mathrm{Re}(\lambda)$ (left) and $\mathrm{Im}(\lambda)$ (right) for Branch 2 which exists exclusively for $\varepsilon \in [\varepsilon_*, 1]$, with $\varepsilon_* \approx 0.90$. Besides three pairs of purely imaginary λ, there is one pair of real exponents and a complex quartet near $\varepsilon = 1$. The pair or real λ corresponds to the numerical results for instability of travelling waves in monomer chains [15] for which instability occurs for $q < 0.9$. The quartet of complex λ gives additional instability, which is not captured by the reductions to the monomer chains. Several more instabilities arise as ε decreases from $\varepsilon = 1$ for the solutions of Branch 2 due to bifurcations of pairs of purely imaginary exponents λ. Branch 2 is unstable in the entire existence interval $[\varepsilon_*, 1]$.

Figure 4.7 shows the stability of solutions of Branch 1 for $N = 5$ (left) and $N = 6$ (right). These figures are included to illustrate the safe splitting of purely imaginary exponents λ near $\varepsilon = 0$ as well as safe coalescence of purely imaginary exponents λ of opposite Krein signature (i.e. coalescence never results in the occurrence of a complex exponent λ). For $N = 5$ and $N = 6$, the solution of Branch 1 remains stable for all $\varepsilon \in [0, 1]$. The predictions from roots of the characteristic polynomial (3.28) are shown by solid lines.

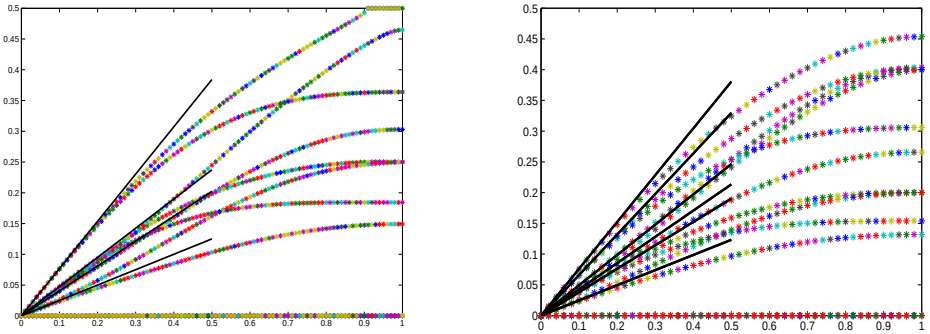

Figure 4.7: Imaginary parts of the characteristic exponents λ versus ε for $N = 5$ (left) and $N = 6$ (right). The real part of all the exponents is zero.

4.3 Gauss-Newton Iterations

While the shooting method shows accurate approximations and agreement with asymptotic approximations for small ε, an alternative numerical method is available to reduce computational time. This numerical method was developed by James [15].

We note that in order to further decrease q using the shooting method, we would require a system of $N = \frac{\pi}{q}$ equations evaluated on the interval $[0, \pi]$. It is evident that, as we approach the limit $q = 0$, the shooting method will become increasingly complex, slow and error prone.

On the other hand the alternative method of James [15] is very robust as it takes full advantage of the travelling wave conditions (4.4) of the system of differential equations (4.1) in order to continue the solution obtained on an interval $[0, 2q]$ to the full period $[0, 2\pi]$. We shall extend the method to the dimer chains.

Let us define the solution to (4.1) as

$$X(t) = [X_1, X_2, \cdots, X_N]^T, \quad X_n = [u_{2n-1}, \dot{u}_{2n-1}, w_{2n}, \dot{w}_{2n}]^T, \tag{4.14}$$

We use the built-in MATLAB function `ode113` to compute the solution $X(t)$ on the interval $[0, 2q]$ where $q = \frac{\pi}{N}$. Let S be a shift operator defined such that

$$S[X_1, X_2, \cdots, X_{N-1}, X_N]^T = [X_2, X_3, \cdots, X_N, X_1]^T. \tag{4.15}$$

We now constrain a solution to (4.1) by the conditions

$$F_{2q} = SX(2q) - X(0) = 0, \tag{4.16}$$

which are equivalent to the travelling wave reduction at $t = 2q = \frac{2\pi}{N}$:

$$\begin{aligned} u_{2n+1}(t) &= u_{2n-1}\left(t - \tfrac{2\pi}{N}\right), \\ w_{2n+2}(t) &= w_{2n}\left(t - \tfrac{2\pi}{N}\right), \end{aligned} \quad t \in \mathbb{R}, \quad 1 \le n \le N. \tag{4.17}$$

We note that these conditions are opposite to the travelling wave conditions (1.12) used earlier. In other words, instead of finding left-travelling waves, the conditions (4.16) allow us to find right-travelling waves. We can circumvent this through the transformation,

$$u(t; -q) = -u(t + \pi; q), \quad w(t; -q) = -w(t + \pi; q), \quad t \in \mathbb{R}, \quad q > 0, \tag{4.18}$$

which connect left-travelling and right-travelling solutions to (4.1). We linearize the system (4.1), and obtain the system (4.3), to compute the matrix DF_{2q}, where the columns of DF_{2q} are given by the partial derivatives of F_{2q} with respect to initial conditions $X(0)$.

We would like to use Gauss-Newton iterations [7] to find zeros of F_{2q} in order to approximate a solution to (4.1). The matrix DF_{2q} is not invertible, and so we exploit the symmetries between solutions to (4.1). These symmetries are equivalent to those found in (4.7) in the case $N = 2$, (4.10) in the case $N = 3$, and (4.13) in the case $N = 4$.

When computing columns of the matrix DF_{2q}, we use columns of the identity matrix as initial conditions to the linearized system (4.3). However, in doing this we do not account for symmetries such as (4.7),(4.10) and (4.13), which lead to a redundancy in parameters in our initial conditions. In order to reduce the number of parameters and to include these symmetries, we introduce the matrix T_N.

While the code for finding T_N for any N can be found in the MATLAB codes for the Gauss-Newton method, we give here the example of T_2 ($N = 2$):

$$T_2 = \begin{bmatrix} 0 & 0 & 0 & 0 \\ 1 & 0 & 0 & 0 \\ 0 & 1 & 0 & 0 \\ 0 & 0 & 1 & 0 \\ 0 & 0 & 0 & 0 \\ 0 & 0 & 0 & 1 \\ 0 & -1 & 0 & 0 \\ 0 & 0 & 1 & 0 \end{bmatrix}$$

This matrix encodes the fact that we have four parameters in the initial con-

ditions after the symmetries (4.7) have been accounted for:

$$u_1(0) = 0, \quad \dot{u}_1(0) = a_1, \quad w_2(0) = a_2, \quad \dot{w}_2(0) = a_3,$$
$$u_3(0) = 0, \quad \dot{u}_3(0) = a_4, \quad w_4(0) = -a_2, \quad \dot{w}_4(0) = a_3.$$

It is clear that $X(0) = T_2\mathbf{a}$, where $\mathbf{a} = [a_1, a_2, a_3, a_4] \in \mathbb{R}^4$.

The Gauss-Newton iterations for a fixed N are used to refine our parameters, $\mathbf{a}$:

$$\mathbf{a}_{new} = \mathbf{a}_{old} - (J_N^T J_N)^{-1} J_N^T F_{2q} \tag{4.19}$$

where $4N \times 2N$ matrix J_N is given by

$$J_N = DF_{2q} * T_N.$$

Since this matrix now accounts for all symmetries of the system (4.1) and has full column rank, the $2N \times 2N$ matrix $J_N^T J_N$ is invertible.

The matrix

$$D_{2q} = DF_{2q} + I = DSX(2q) = \begin{pmatrix} \frac{\partial X_2(2q)}{\partial X_1(0)} & \cdots & \frac{\partial X_2(2q)}{\partial X_N(0)} \\ \vdots & \ddots & \vdots \\ \frac{\partial X_1(2q)}{\partial X_1(0)} & \cdots & \frac{\partial X_1(2q)}{\partial X_N(0)} \end{pmatrix}$$

is said to be related to the monodromy matrix [15] but a proof of this fact is not offered in [15]. We state and prove the following theorem.

Theorem 3. *Consider the solution to system* (4.1) *with* $q = \frac{\pi}{N}$, *organized in the blocks* (4.14). *Let* $R(t, t_0)$ *be the fundamental matrix solution to the*

linearized system (4.3)*, where* t_0 *is the initial time. Then we have,*

$$D_{2q} = SR(2q; 0), \tag{4.20}$$

$$SR(t + 2q; t_0) = R(t; t_0 - 2q)S, \tag{4.21}$$

and

$$R(2\pi; 0) = [D_{2q}]^N \tag{4.22}$$

Remark 10. *By Theorem 3, we only need a solution to the nonlinear system* (4.1) *on the interval* $[0, 2q]$ *in order to obtain numerical results for stability of periodic travelling waves. In the limit of small* q*, we should expect more accurate results than the shooting method, as well as a decrease in the computational time.*

Proof. We prove equation (4.20) by considering the first column of D_{2q},

$$[D_{2q}]_1 = \begin{bmatrix} \frac{\partial X_2(2q)}{\partial X_1(0)} \\ \vdots \\ \frac{\partial X_N(2q)}{\partial X_1(0)} \\ \frac{\partial X_1(2q)}{\partial X_1(0)} \end{bmatrix} = S \begin{bmatrix} \frac{\partial X_1(2q)}{\partial X_1(0)} \\ \vdots \\ \frac{\partial X_{N-1}(2q)}{\partial X_1(0)} \\ \frac{\partial X_N(2q)}{\partial X_1(0)} \end{bmatrix} = S\left[Y(2q)\right]_1,$$

where the first column $[Y(t)]_1$ is the derivative of the solution vector $X(t)$ with respect to $X_1(0)$. The column $[Y]_1$ solves the linearized system (4.3) with initial data being an identity block for the first entry of $[Y(0)]_1$. In other words, $[Y]_1$ is the first column of the monodromy matrix for the linearized system (4.3) and hence $D_{2q} = SR(2q; 0)$ is proved for the first column. Generalizing this for any column, equation (4.20) is proved for the entire matrix.

Next, we prove equation (4.21); for simplicity we take $t_0 = 0$.

Notice that each column of $R(t; 0)$ solves the linearized system with

initial data $R(0,0) = I$, where I is the identity. Let us denote $Z(t) = SR(t + 2q; 0)$. Therefore, $Z(t)$ solves the linearized system (4.3) with initial condition $Z(0) = SR(2q; 0)$. By the travelling wave reduction, we have $X_n(t) = X_{n-1}(t-2q)$. As a result, we have

$$[Z(t)]_1 = \begin{bmatrix} \frac{\partial X_2(t+2q)}{\partial X_1(0)} \\ \vdots \\ \frac{\partial X_N(t+2q)}{\partial X_1(0)} \\ \frac{\partial X_1(t+2q)}{\partial X_1(0)} \end{bmatrix} = \begin{bmatrix} \frac{\partial X_1(t)}{\partial X_N(-2q)} \\ \vdots \\ \frac{\partial X_{N-1}(t)}{\partial X_N(-2q)} \\ \frac{\partial X_N(t)}{\partial X_N(-2q)} \end{bmatrix} = [R(t;-2q)]_N = [R(t;-2q)S]_1$$

Therefore $Z(t) = R(t;-2q)S$ is proved for the first column and similarly for any column. Hence, equation (4.21) is proved for the entire matrix $Z(t)$.

To prove equation (4.22), we expand $[D_{2q}]^N$, using equations (4.20) and (4.21):

$$\begin{aligned} [D_{2q}]^N &= [SR(2q;0)]^N \\ &= SR(2q;0)SR(2q;0)...SR(2q;0)SR(2q;0) \\ &= SR(2q;0)...SR(2q;0)SSR(4q;2q)R(2q;0) \\ &\vdots \\ &= S^N R(2Nq;2(N-1)q)...R(6q;4q)R(4q;2q)R(2q;0) \\ &= R(2Nq;0) \\ &= R(2\pi;0). \end{aligned}$$

In the second last equation, we have used two results. First, $S^N = I$, by the construction of S. Second, each monodromy matrix in the chain

$$R(2Nq;2(N-1)q)...R(6q;4q)R(4q;2q)R(2q;0)$$

computes the fundamental solution on an interval of length $2q$, starting at the end point of the previous matrix. Therefore, together they give $R(2Nq; 0) = R(2\pi; 0)$. □

Table 5.2 compares computational time in seconds for the shooting method and the Gauss-Newton method described here for $N = 3$ and $N = 4$. The time represents the time taken by a 3.2GHz Pentium M processor working with 2GB of RAM to approximate solutions and characteristic exponents for the solution of Branch 2 at $\varepsilon = 1$. We can see that the Gauss-Newton method is faster than the shooting method. Again, this is obvious considering the fact that we are approximating a solution on a smaller interval, $[0, 2q]$.

N	Elapsed time of shooting method	Elapsed time of Gauss-Newton method
3	$73s$	$46s$
4	$206s$	$114s$

Table 5.2: Comparison of computational time for the shooting method and the Gauss-Newton method for $N = 3$ and $N = 4$.

An additional advantage of the Gauss-Newton method is that we only need to use the ODE solver once to compute both the solution of the nonlinear system (4.1) and the characteristic exponents of the linearized system (4.3). On comparison, in the shooting method we need to use the ODE solver to approximate the solution of the nonlinear system (4.1) on the interval $[0, \pi]$ and again to compute the characteristic exponents of the linearized system (4.3) on the full period $[0.2\pi]$.

4.4 Stability of Uniform Periodic Oscillations

The periodic solution with $q = 0$ (which is no longer a travelling wave but a uniform oscillation of all sites of the dimer) is given by the exact solution (1.27). Spectral stability of this solution is obtained from the system of linearized equations (3.3). Using the boundary conditions

$$u_{2n+1} = e^{2i\theta} u_{2n-1}, \quad w_{2n+2} = e^{2i\theta} w_{2n}, \quad n \in \mathbb{Z},$$

where $\theta \in [0, \pi]$ is a continuous parameter, we obtain the system of two closed second-order equations,

$$\begin{cases} \ddot{u} + \frac{\alpha}{1+\varepsilon^2} |\varphi|^{\alpha-1} u = \frac{\varepsilon}{1+\varepsilon^2} \left(V''(-\varphi) + V''(\varphi) e^{-2i\theta} \right) w, \\ \ddot{w} + \frac{\alpha\varepsilon^2}{1+\varepsilon^2} |\varphi|^{\alpha-1} w = \frac{\varepsilon}{1+\varepsilon^2} \left(V''(-\varphi) + V''(\varphi) e^{2i\theta} \right) u. \end{cases} \tag{4.23}$$

The characteristic equation (3.28) for $q = 0$ predicts a double pair (3.9) of purely imaginary Λ for any $\theta \in (0, \pi)$. We confirm here numerically that the double pair is preserved for all $\varepsilon \in [0, 1]$.

Figure 4.8 shows the imaginary part of the characteristic exponents λ of the linearized system (4.23) for $\theta = \frac{\pi}{2}$ (left) and $\theta = \frac{\pi}{4}$ (right). Similar results are obtained for other values of θ. Therefore, the periodic solution with $q = 0$ remains stable for all values of $\varepsilon \in [0, 1]$.

The pattern on Figure 4.8 suggests a hidden symmetry in this case. Suppose λ_θ is a characteristic exponent of the system (4.23) for the eigenvector

$$\begin{bmatrix} u \\ w \end{bmatrix} = \begin{bmatrix} U_\theta(t) \\ W_\theta(t) \end{bmatrix} e^{\lambda_\theta t}, \tag{4.24}$$

where $U_\theta(t)$ and $W_\theta(t)$ are 2π-periodic and the subscript θ indicates that the

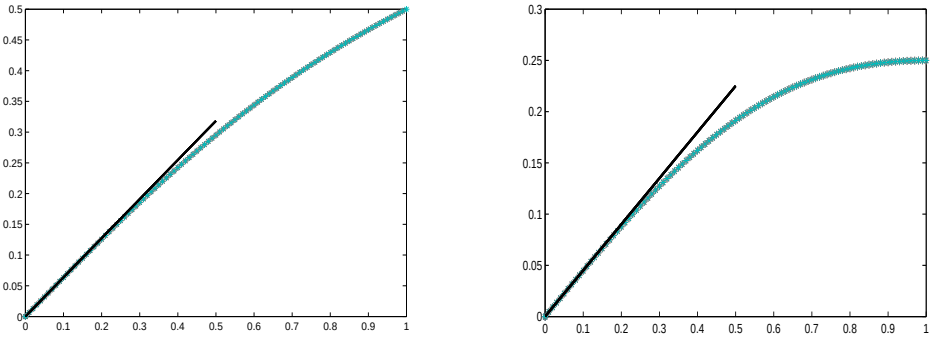

Figure 4.8: Imaginary parts of the characteristic exponents λ versus ε for $\theta = \frac{\pi}{2}$ (left) and $\theta = \frac{\pi}{4}$ (right). The real part of all the exponents is zero.

system (4.23) depends explicitly on θ. Recall that the unperturbed solution satisfies the symmetry $\varphi(t+\pi) = -\varphi(t)$ for all t. Using this symmetry and the trivial identity $e^{2\pi i} = 1$, we can verify that there is another solution of the system (4.23) with the same θ for the characteristic exponent $\lambda_{\pi-\theta}$:

$$\begin{bmatrix} u \\ w \end{bmatrix} = \begin{bmatrix} U_{\pi-\theta}(t+\pi) \\ e^{2i\theta} W_{\pi-\theta}(t+\pi) \end{bmatrix} e^{\lambda_{\pi-\theta} t}. \tag{4.25}$$

From the symmetry of roots (3.9) and the corresponding characteristic exponents, we have $\lambda_\theta = \lambda_{\pi-\theta}$. The eigenvectors (4.24) and (4.25) are generally linearly independent and coexist for the same value of $\lambda = \lambda_\theta = \lambda_{\pi-\theta}$. This argument explains the double degeneracy of characteristic exponents λ for the case $q = 0$ for all values of $\varepsilon \in [0, 1]$.

Conclusions and Open Problems

We have studied periodic travelling waves in granular dimer chains by continuing solutions from the anti-continuum limit (i.e. when the mass ratio between the light and heavy particles is zero). We have shown that the limiting periodic waves are all uniquely continued from the anti-continuum limit for small mass ratio parameters. Despite the lack of smoothness of vector fields of the granular dimer chains, we are still able to use the implicit function theorem to guarantee a C^1 continuation with respect to the mass ratio parameter. Rigorous perturbation theory is used to compute characteristic exponents in the linearized stability problem. We are able to show that periodic waves with wavelengths larger than a certain critical value are spectrally stable for small mass ratios.

We have used numerical techniques to show that for larger wavelengths the stability of these periodic travelling waves persists all the way to the limit of equal mass ratio. We also compute periodic travelling waves continued from the solutions of granular monomer chains at the equal mass ratio, their spectral stability and their termination points with respect to mass ratio parameter.

There are several open questions which are left for further studies. The nature of the bifurcations where Branch 2 terminates at $\varepsilon_* \in (0, 1)$ needs to be clarified. We have been unsuccessful in our attempts to find another solution

branch nearby for $\varepsilon \gtrapprox \varepsilon_*$. The safe coalescence of purely imaginary characteristic exponents λ of opposite Krein signatures is also remarkable. We are still lacking understanding the hidden symmetry in the linearized stability problem that would explain why the eigenvalues at the coalescence point remain semi-simple.

MATLAB Codes

This script was used to compute solutions and characteristic exponents for the case $N = 4$ using the shooting method. Similar codes exist for $N = 2, 3$.

```
function Dim_FM8
clear all
tic
p=8;
eps = 1;
nn=1;
options = odeset('RelTol',1e-12,'AbsTol',1e-12);
%a=([0 1.1278 0 0 1.2038 0.0000 0 0  0 -1.1278 0 0 -1.2038 0.0000 0 0])';
a=([0 2.2030 1.7302 2.2030 3.4605 2.2030 4.9781 0.4028 0  -11.8207
    -4.9781    0.4028   -3.4605    2.2030 -1.7302    2.2030])';
v1=[0,1,0,0,0,0,0,0,0,0,0,0,0,0,0,0]';
v2=[0,0,1,0,0,0,0,0,0,0,0,0,0,0,-1,0]';
v3=[0,0,0,1,0,0,0,0,0,0,0,0,0,0,0,1]';
v4=[0,0,0,0,1,0,0,0,0,0,0,0,-1,0,0,0]';
v5=[0,0,0,0,0,1,0,0,0,0,0,0,0,1,0,0]';
v6=[0,0,0,0,0,0,1,0,0,0,-1,0,0,0,0,0]';
v7=[0,0,0,0,0,0,0,1,0,0,0,1,0,0,0,0]';
v8=[0,0,0,0,0,0,0,0,0,1,0,0,0,0,0,0]';
for eps=1:-0.002:1
aa=zeros(16,1);
while (norm(aa-a) > 1e-10)
T=pi;
aa=a;
ic =[a;v1;v2;v3;v4;v5;v6;v7;v8];
[~,x] = ode45(@DIM,[0,pi/2,T],ic,options);
n_t=length(x(:,1));
n2=2;
F=[x(n_t,1),x(n_t,3)+x(n_t,15),x(1,3)-x(n_t,11),
```

```
    x(n_t,5)+x(2,1),x(1,5)-x(n_t,13),x(n_t,7)+x(n_t,11),
    x(1,15)-x(n_t,7),x(n_t,9)];
for k1=1:8
DF(k1,:)=[x(n_t,1+k1*16),x(n_t,3+k1*16)+x(n_t,15+k1*16),
  x(1,3+k1*16)-x(n_t,11+k1*16),x(n_t,5+k1*16)+x(2,1+k1*16),
  x(1,5+k1*16)-x(n_t,13+k1*16),x(n_t,7+k1*16)+x(n_t,11+k1*16),
  x(1,15+k1*16)-x(n_t,7+k1*16),x(n_t,9+k1*16)];
end
DF=transpose(DF);
a=([a(2),a(3),a(4),a(5),a(6),a(7),a(8),a(10)])'-DF\F';
a=([0,a(1),a(2),a(3),a(4),a(5),a(6),a(7),
    0,a(8),-a(6),a(7),-a(4),a(5),-a(2),a(3)])';
norm(aa-a)
end
[t,x] = ode45(@DIM,[0 2*T],ic,options);
figure(6)
plot(t,[x(:,1),x(:,3),x(:,5),x(:,7),x(:,9),x(:,11),x(:,13),x(:,15)])
T=2*pi;
for jj=1:16
ic=zeros(32,1);
ic(1:16)=a;
ic(16+jj)=1;
[tt,xx] = ode45(@DIM_lin,[0,T],ic,options);
n_time = length(xx(:,1));
M(:,jj) = (xx(n_time,17:32))';
end
figure(2)
plot(tt,xx(:,1))
hold on
eps
EM=eig(M)
for j=1:16
Enorm(j)=norm(EM(j));
end
Emax(nn)=max(Enorm);
figure(3)
plot(cos(tt),sin(tt))
hold on
plot(real(EM),imag(EM),'r*')
nn=nn+1;
figure(1)
plot(eps,x(1,3),'*')
```

```
hold on
epsil(nn)=(eps);
EM=sort(EM)
FM(:,nn)=abs(EM);
FMa=angle(EM);
FM1(:,nn)=FMa;
nn=nn+1;
end
a'
Y=(log(FM))/(2*pi);
figure(7)
plot(epsil,Y,'*')
figure(8)
plot(epsil,FM1/(2*pi),'*')
toc
function y = f(x)
if(x>0)
y=(x)^(3/2);
else
y=0;
end
end
function y=df(x)
if(x>0)
y=(3/2)*sqrt(x);
else
y=0;
end
end

function dx = DIM(~,x)
dx=zeros(2*p+2*(p)^2,1);
for i1=1:2:2*p-1
dx(i1)=x(i1+1);
end
for i1=4:4:2*p-2
dx(i1)=(eps*(f(x(i1-3)-eps*x(i1-1))-f(eps*x(i1-1)-x(i1+1))));
end
for i1=6:4:2*p-2
dx(i1)=(f(eps*x(i1-3)-x(i1-1))-f(x(i1-1)-eps*x(i1+1)));
end
for i1=2
```

```
dx(i1)=(f(eps*x(2*p-1)-x(1))-f(x(1)-eps*x(3)));
dx(2*p)=(eps*(f(x(2*p-3)-eps*x(2*p-1))-f(eps*x(2*p-1)-x(1))));
end
for j1=1:p
for i2=1+2*p*j1:2:2*p-1+2*p*j1
dx(i2)=x(i2+1);
end
for i2=4+2*p*j1:4:2*p-2+2*p*j1
dx(i2)=(eps*(df(x(i2-3-2*p*j1)-eps*x(i2-1-2*p*j1))*(x(i2-3)-eps*x(i2-1))
    -df(eps*x(i2-1-2*p*j1)-x(i2+1-2*p*j1))*(eps*x(i2-1)-x(i2+1))));
end
for i2=6+2*p*j1:4:2*p-2+2*p*j1
dx(i2)=(df(eps*x(i2-3-2*p*j1)-x(i2-1-2*p*j1))*(eps*x(i2-3)-x(i2-1))
    -df(x(i2-1-2*p*j1)-eps*x(i2+1-2*p*j1))*(x(i2-1)-eps*x(i2+1)));
end
for i2=2+2*p*j1
dx(i2)=(df(eps*x(2*p-1)-x(1))*(eps*x(2*p-1+2*p*j1)-x(i2-1))-df(x(1)
    -eps*x(3))*(x(i2-1)-eps*x(i2+1)));
dx(2*p*j1+2*p)=(eps*(df(x(2*p-3)-eps*x(2*p-1))*(x(2*p*j1+2*p-3)
    -eps*x(2*p*j1+2*p-1))-df(eps*x(2*p-1)-x(1))*(eps*x(2*p+2*p*j1-1)
    -x(2*p*j1+1))));
end
end
end
function dx = DIM_lin(~,x)
dx = zeros(32,1);
dx(1) = x(2);
dx(2) = f(eps*x(15)-x(1))-f(x(1)-eps*x(3));
dx(3) = x(4);
dx(4) = eps*(f(x(1)-eps*x(3))-f(eps*x(3)-x(5)));
dx(5) = x(6);
dx(6) = f(eps*x(3)-x(5))-f(x(5)-eps*x(7));
dx(7) = x(8);
dx(8) = eps*(f(x(5)-eps*x(7))-f(eps*x(7)-x(9)));
dx(9) = x(10);
dx(10) =f(eps*x(7)-x(9))-f(x(9)-eps*x(11));
dx(11) = x(12);
dx(12) = eps*(f(x(9)-eps*x(11))-f(eps*x(11)-x(13)));
dx(13) = x(14);
dx(14) = f(eps*x(11)-x(13))-f(x(13)-eps*x(15));
dx(15) = x(16);
dx(16) = eps*(f(x(13)-eps*x(15))-f(eps*x(15)-x(1)));
```

```
for jk=0
dx(17+jk*16) = x(18+jk*16);
dx(18+jk*16) = df(eps*x(15)-x(1))*(eps*x(31+jk*16)-x(17+jk*16))-df(x(1)
-eps*x(3))*(x(17+jk*16)-eps*x(19+jk*16));
dx(19+jk*16) = x(20+jk*16);
dx(20+jk*16) = eps*(df(x(1)-eps*x(3))*(x(17+jk*16)-eps*x(19+jk*16))
-df(eps*x(3)-x(5))*(eps*x(19+jk*16)-x(21+jk*16)));
dx(21+jk*16) = x(22+jk*16);
dx(22+jk*16) = df(eps*x(3)-x(5))*(eps*x(19+jk*16)-x(21+jk*16))-df(x(5)
-eps*x(7))*(x(21+jk*16)-eps*x(23+jk*16));
dx(23+jk*16) = x(24+jk*16);
dx(24+jk*16) = eps*(df(x(5)-eps*x(7))*(x(21+jk*16)-eps*x(23+jk*16))
-df(eps*x(7)-x(9))*(eps*x(23+jk*16)-x(25+jk*16)));
dx(25+jk*16) = x(26+jk*16);
dx(26+jk*16) = df(eps*x(7)-x(9))*(eps*x(23+jk*16)-x(25+jk*16))-df(x(9)
-eps*x(11))*(x(25+jk*16)-eps*x(27+jk*16));
dx(27+jk*16) = x(28+jk*16);
dx(28+jk*16) = eps*(df(x(9)-eps*x(11))*(x(25+jk*16)-eps*x(27+jk*16))
-df(eps*x(11)-x(13))*(eps*x(27+jk*16)-x(29+jk*16)));
dx(29+jk*16) = x(30+jk*16);
dx(30+jk*16) = df(eps*x(11)-x(13))*(eps*x(27+jk*16)-x(29+jk*16))
-df(x(13)-eps*x(15))*(x(29+jk*16)-eps*x(31+jk*16));
dx(31+jk*16) = x(32+jk*16);
dx(32+jk*16) = eps*(df(x(13)-eps*x(15))*(x(29+jk*16)-eps*x(31+jk*16))
-df(eps*x(15)-x(1))*(eps*x(31+jk*16)-x(17+jk*16)));
end
end

end
```

This script computes solutions and characteristic exponents for the case $N = 3$ using the Gauss-Newton method.

```
 function GNdim
tic
eps=0.1;
p=6; %p=2N
m=1;
n=2400;
fixed=linspace(0,1,n+1)*(pi);
q=4*m*pi/p;
nn=1;
kk=1;
```

```
options = odeset('RelTol',2.3e-14,'AbsTol',1e-15);
%a=[0,u0(1,2),-u0(600,1),u0(600,2),0,u0(1200,2),u0(600,1),u0(600,2)]';
%p=6
a=[0 0.8905 0.9322 0.8905 1.8089 0.4563 0 -3.5842
      -1.8089 0.4563 -0.9325    0.8905]';
%a=([0,1.1278,0,0,1.0293,-0.6418,0,0,-1.0293,-0.6418,0,0])'; %Main Branch
%p=4
%a=([0,1.127491828593248,0,0,0,-1.127491828593248,0,0])';
%a=([0,0.7795,-0.4599,-0.2412,0,-0.2973,0.4599,-0.2412])';
%a=([-0.0000,0.2973,0.4599,-0.2412,0,-0.7795,-0.4599,-0.2412])';
%p=8
%a=([0 1.1278 0 0 1.2038 0 0 0  0 -1.1278 0 0 -1.2038 0.0 0 0])';
%a=([0 2.2030 1.7302 2.2030 3.4605 2.2030 4.9781 0.4028 0 -11.8207 -4.9781
      0.4028 -3.4605 2.2030 -1.7302 2.2030])';
%p=10
%a=([0 1.1278 0 0 -1.1395 0.4039 0 0 -0.6821 -0.9821
      0 0 0.6821 -0.9821 0 0 1.1395 0.4039 0 0])';
%a=[0   31.1444  -11.1504    0.7632   -8.7976   -4.6673   -5.8650
    -4.6673 -2.9325   -4.6673  0   -4.6673    2.9325   -4.6673 5.8650
    -4.6673 8.7976   -4.6673 11.1504 0.7632 ])';
%p=12
%a=([0 1.1278 0 0 -1.0293 0.6418 0 0 -1.0293 -0.6418
      0 0 0 -1.1278 0 0 1.0293 -0.6418  0 0 1.0293 0.6418 0 0])';
%a=([0 70.2179 -21.7997 4.5955 -18.4793 -8.8232 -13.8595 -8.8232 -9.2396
      -8.8232 -4.6198 -8.8232 0 -8.8232 4.6198 -8.8232 9.2396 -8.8232
      13.8595 -8.8232 18.4793 -8.8232 21.7997 4.5955])';
S=eye(2*p,2*p);
 S=circshift(S,[0 4])
 S1=eye(2*p,2*p);
 S1=circshift(S,[0 -2])
T=eye(2*p,p);
T=circshift(T,[1,0]);
T(p+1,p)=0;
T(p+2,p)=1;
for pp=1:2:p-2
    T(p*2-pp,pp+1)=-1;
end
for pp=0:2:p-3
    T(2*p-pp,pp+3)=1;
end
 v=eye(2*p,2*p);
for eps=1:0.02:1
```

```
    aa=zeros(2*p,1);
while (norm(aa-a)>1e-12) && (norm(aa-a)<1000)
    aa=a;
    ic(1:2*p,1)=a;
    for j=1:2*p
        ic(2*p*j+1:2*p*(j+1),1)=v(:,j);
    end
    [t,x] = ode113(@DIM,[0 q],ic,options);
    nt=length(x(:,1));
    F=zeros(nt);
    F1=[x(1,1:2*p)]';
    F2=[x(nt,1:2*p)]';
    F=(F2-S*F1);
    DF=zeros(2*p,2*p);
    for jj=1:2*p
        F3=[x(1,1+jj*2*p:2*p*(jj+1))]';
        F4=[x(nt,1+jj*2*p:2*p*(jj+1))]';
        F5=[x(2,1+jj*2*p:2*p*(jj+1))]';
        DF(:,jj)=(F4-S*F3);
    end
    M=DF+v;
    DF=DF*T;
    DFT=transpose(DF);
    a1=zeros(p,1);
    for i=1:p-1
        a1(i)=a(i+1);
    end
    a1(p)=a(p+2);
    a1=a1-(DFT*DF)\(DFT*F);
    for i=1:p-1
        a(i+1)=a1(i);
    end
    a(1)=0;
    a(p+1)=0;
    a(p+2)=a1(p);
    for i=1:2:p-2
        a(2*p-i+1)=a1(i+2);
    end
    for i=1:2:p-2
        a(2*p-i)=-a1(i+1);
    end
    norm(aa-a)
```

```
end
a'

M=M^(p/2);
figure(1)
plot(eps,x(1,3),'*')
% hold on
 figure(2)
 plot(t,[x(:,1),x(:,3),x(:,5),x(:,7)]);
 hold on
[V,EM]=eig(M);
EM=eig(M);

     time=[0:pi/20:2*pi];
     figure(4)
     plot(cos(time),sin(time))
     hold on
     plot(real(EM),imag(EM),'r*')
     hold on
epsil(nn)=(eps);
EM=sort(EM)
FM(:,nn)=real(EM);
FMa=angle(EM);
FM1(:,nn)=FMa;
nn=nn+1;
end
figure(12)
plot(t,[x(:,1),x(:,3),x(:,5),x(:,7),x(:,9),x(:,11)]);
hold on
plot(t+q,[x(:,5),x(:,7),x(:,9),x(:,11),x(:,1),x(:,3)]);
plot(t+2*q,[x(:,9),x(:,11),x(:,1),x(:,3),x(:,5),x(:,7)]);
B(:,1)=ones(nn-1,1);
B(:,2)=epsil;
Y=(log(FM))/(2*pi);
% XCX=B\Y.'
% Err=B*XCX-Y.'
figure(7)
plot(epsil,Y,'*')
figure(8)
plot(epsil,FM1/(2*pi),'*')
legend('Real','Imag','RD','IMD')
% figure(3)
```

```
% plot(1:-0.001:0.984,Enorm)
toc
function y = f(x)
if(x>0)
y=(x)^(3/2);
else
y=0;
end
end
function y=df(x)
if(x>0)
y=(3/2)*sqrt(x);
else
y=0;
end
end
function dx = DIM(~,x)
dx=zeros(2*p+(2*p)^2,1);
for i1=1:2:2*p-1
dx(i1)=x(i1+1);
end
for i1=4:4:2*p-2
dx(i1)=(eps*(f(x(i1-3)-eps*x(i1-1))-f(eps*x(i1-1)-x(i1+1))));
end
for i1=6:4:2*p-2
dx(i1)=(f(eps*x(i1-3)-x(i1-1))-f(x(i1-1)-eps*x(i1+1)));
end
for i1=2
dx(i1)=(f(eps*x(2*p-1)-x(1))-f(x(1)-eps*x(3)));
dx(2*p)=(eps*(f(x(2*p-3)-eps*x(2*p-1))-f(eps*x(2*p-1)-x(1))));
end
for j1=1:2*p
for i2=1+2*p*j1:2:2*p-1+2*p*j1
dx(i2)=x(i2+1);
end
for i2=4+2*p*j1:4:2*p-2+2*p*j1
dx(i2)=(eps*(df(x(i2-3-2*p*j1)-eps*x(i2-1-2*p*j1))*(x(i2-3)-eps*x(i2-1))
      -df(eps*x(i2-1-2*p*j1)-x(i2+1-2*p*j1))*(eps*x(i2-1)-x(i2+1))));
end
for i2=6+2*p*j1:4:2*p-2+2*p*j1
dx(i2)=(df(eps*x(i2-3-2*p*j1)-x(i2-1-2*p*j1))*(eps*x(i2-3)-x(i2-1))
      -df(x(i2-1-2*p*j1)-eps*x(i2+1-2*p*j1))*(x(i2-1)-eps*x(i2+1)));
```

```
end
for i2=2+2*p*j1
dx(i2)=(df(eps*x(2*p-1)-x(1))*(eps*x(2*p-1+2*p*j1)-x(i2-1))-df(x(1)
      -eps*x(3))*(x(i2-1)-eps*x(i2+1)));
dx(2*p*j1+2*p)=(eps*(df(x(2*p-3)-eps*x(2*p-1))*(x(2*p*j1+2*p-3)
     -eps*x(2*p*j1+2*p-1))-df(eps*x(2*p-1)-x(1))*(eps*x(2*p+2*p*j1-1)
      -x(2*p*j1+1))));
end
end
end
end
```

This script computes the numerical constants of the characteristic equation (3.28).

```
 function Phase
dphi0=1.127781604466791;
%Input desired 0=<q=<pi/2
q=pi/6;
Theta0=pi/4;
%---------------------------------
mnum=(2*n1/pi)*q;
M2=M2data(n1-mnum)
Cp=-u0(1,2)/pi;
Cm=-Cp;
E0=(dphi0^2)/2;
Tprime=-0.9894;
K=-(2*pi)^2/Tprime
M1=2/(pi*(dphi0)^2*Tprime)
L1=(2*(2*pi-Tprime*dphi0^2))/(Tprime*dphi0)
L2=L1/(2*pi);
C=(K*M1+L1*L2+M2);
Delta=4*K*M1*M2;
M0=-4*E0/pi;
C0=(K*M1+L1*L2+M0);
D0=4*K*M1*M0;
D=[K,0,4*(sin(Theta0))^2*C,0,4*(sin(Theta0)^4)*Delta/K];
LA1=[sqrt(-(2/K)*C+sqrt((4/K^2)*(C^2-Delta)));\
      -sqrt(-(2/K)*C+sqrt((4/K^2)*(C^2-Delta)));sqrt(-(2/K)*C
      -sqrt((4/K^2)*(C^2-Delta)));-sqrt(-(2/K)*C-sqrt((4/K^2)
      *(C^2-Delta)))]
LA0=[K,0,4*(sin(Theta0))^2*C0,0,4*(sin(Theta0)^4)*D0/K];
CE0=roots(LA0)
```

```
te=[0:0.01:0.5];
KK=roots(D)
figure(7)
plot(te,imag(CE0)*te ,'k','LineWidth',2)
 hold on
 plot(te,imag(CE0)*te ,'k','LineWidth',2)
end
```

This script computes the periodic solution and characteristic exponents for $q = 0$.

```
 function Qzero
 alpha=3/2;
 theta=pi/4;
 options = odeset('RelTol',1e-12,'AbsTol',1e-15);
 ic=eye(4,4);
 a=[0,1.127781604466791]';
 nn=1;
 for eps=0:0.01:1
 for j=1:4
 [t,x]=ode113(@DIM,[0 2*pi],[a;ic(:,j)],options,alpha,eps);
 x_l=length(x(:,1));
 M(:,j)=x(x_l,3:6);
 figure(1)
 plot(t,x(:,3),'b',t,x(:,5),'r')
 hold on
 end
 EM=eig(M);
 [D,V]=eig(M)
epsil(nn)=(eps);
EM=sort(EM)
FMa(:,nn)=angle(EM);
FMa=sort(FMa);

nn=nn+1;
 end
B(:,1)=ones(nn-1,1);
B(:,2)=epsil;
figure(7)
plot(epsil,[FMa/(2*pi)],'*')
  function y = f(x)
        if(x>0)
            y=(x)^(alpha);
```

```
        else
            y=0;
        end
    end
 function y = df(x)
        if(x>0)
            y=(x)^(alpha-1);
        else
            y=0;
        end
    end
 function dx = DIM(~,x,alpha,eps)
     dx=zeros(6,1);
      dx(1)=x(2);
      dx(2)=-x(1)*sqrt(abs(x(1)));
    dx(3)=x(4);
    dx(4)=(eps*alpha/(1+eps^2))
  *(df(-x(1))+df(x(1))*exp(-2*sqrt(-1)*theta))*(x(5))
  -((alpha*sqrt(abs(x(1))))/(1+eps^2))*(x(3));
    dx(5)=x(6);
    dx(6)=(eps*alpha/(1+eps^2))
*(df(-x(1))+df(x(1))*exp(2*sqrt(-1)*theta))*(x(3))
-((eps^2*alpha*sqrt(abs(x(1))))/(1+eps^2))*(x(5));
 end
end
```

Bibliography

[1] K. Ahnert and A. Pikovsky, "Compactons and chaos in strongly nonlinear lattices", Phys. Rev. E **79** (2009), 026209 (10 pages).

[2] S. Aubry, "Breathers in nonlinear lattices: Existence, linear stability and quantization", Physica D **103** (1997), 201–250.

[3] T.J. Bridges, "Bifurcation of periodic solutions near a collision of eigenvalues of opposite signature", Math. Proc. Camb. Phil. Soc. **108** (1990), 575–601.

[4] M. Chugunova and D. Pelinovsky, "Count of unstable eigenvalues in the generalized eigenvalue problem", J. Math. Phys. **51** (2010), 052901 (19 pages).

[5] M. Chugunova and D. Pelinovsky, "On quadratic eigenvalue problems arising in stability of discrete vortices", Lin. Alg. Appl. **431** (2009), 962–973.

[6] C. Daraio, V.F. Nesterenko, E.B. Herbold, and S. Jin, "Tunability of solitary wave properties in one-dimensional strongly nonlinear phononic crystals", Phys. Rev. E **73** (2006), 026610 (10 pages).

[7] J.E. Dennis Jr. and R.B. Schnabel, "Numerical methods for unconstrained optimization and nonlinear equations", Prentice-Hall Series in Computational Mathematics, Prentice-Hall (1984).

[8] O. Diekmann, S.A. van Gils, S.M.V. Lunel, and H.-O. Walther, "Delay Equations:Functional-,Complex-, and Nonlinear Analysis", Applied Mathematical Sciences **110**, Springer-Verlag (1995).

[9] J.M. English and R.L. Pego, "On the solitary wave pulse in a chain of beads", Proc. AMS **133** (2005), 1763–1768.

[10] E.I. Fredholm, "Sur une classe d'equations fonctionnelles", Acta Math. **27** (1903), 365–390.

[11] G. Friesecke and J.A.D. Wattis, "Existence theorem for solitary waves on lattices", Comm. Math. Phys. **161** (1994), 391–418.

[12] M. Grasselli and D. Pelinovsky, "Numerical Mathematics", Jones and Bartlett (2008).

[13] U. Harbola, A. Rosas, A.H. Romero, M. Esposito, and K. Lindenberg, "Pulse propagation in decorated granular chains: an analytical approach", Phys. Rev. E **80** (2009), 051302 (9 pages).

[14] G. James, "Nonlinear waves in Newton's cradle and the discrete p-Schrdödinger equation", Math. Models Methods Appl. Sci. **21** (2011), 2335-2377.

[15] G. James, "Periodic travelling waves in granular chains", J. Nonlin. Sci. (2012), in press.

[16] G. James, P.G. Kevrekidis, and J. Cuevas "Breathers in oscillatory chains with Hertzian interactions", Physica D (2012), in press.

[17] K.R. Jayaprakash, Yu. Starosvetsky, and A.F. Vakakis, "New family of solitary waves in granular dimer chains with no precompression", Phys. Rev. E **83** (2011), 036606 (11 pages).

[18] K.R. Jayaprakash, A.F. Vakakis, and Yu. Starosvetsky, "Strongly nonlinear traveling waves in granular dimer chains", Mech. Syst. Sign. Proc. (2012) (27 pages), in press.

[19] R. Kollar, "Homotopy method for nonlinear eigenvalue pencils with applications", SIAM J. Math. Anal. **43** (2011), 612–633.

[20] R.S. MacKay, "Stability of equilibria of Hamiltonian systems", "*Nonlinear phenomenon and chaos*", Malvern Phys. Ser., Hilger, Bristol, (1986), 254–270.

[21] R.S. MacKay, "Solitary waves in a chain of beads under Hertz contact", Phys. Lett. A **251** (1999), 191–192.

[22] D.W. Marquardt, "An algorithm for least-squares estimation of nonlinear parameters", Journal of the Society for Industrial and Applied Mathematics, **11** (1963), 431–441.

[23] D.E. Pelinovsky and A. Sakovich, "Multi-site breathers in Klein–Gordon lattices: stability, resonances, and bifurcations", Nonlinearity (2012), submitted.

[24] M.A. Porter, C. Daraio, I. Szelengowics, E.B. Herbold, and P.G. Kevrekidis, "Highly nonlinear solitary waves in heterogeneous periodic granular media", Physica D **238** (2009), 666–676.

[25] S. Sen, J. Hong, J. Bang, E. Avalos, and R. Doney, "Solitary waves in the granular chain", Phys. Rep. **462** (2008), 21–66.

[26] Yu. Starosvetsky and A.F. Vakakis, "Traveling waves and localized modes in one-dimensional homogeneous granular chains with no precompression", Phys. Rev. E **82** (2010), 026603 (14 pages).

[27] A. Stefanov and P.G. Kevrekidis, "On the existence of solitary traveling waves for generalized Hertzian chains", J. Nonlin. Sci. (2012), in press.

[28] K. Yoshimura, "Existence and stability of discrete breathers in diatomic Fermi–Pasta–Ulam type lattices", Nonlinearity **24** (2011), 293–317.